Zwitterionic Peptide Fusion Proteins for Therapeutic and Protective Applications

Patrick J. McMullen

A dissertation

submitted in partial fulfillment of the

requirements for

Doctor of Philosophy

University of Washington

2020

Reading Committee:

Shaoyi Jiang, Chair

James M. Carothers

David A. Beck

Program Authorized to Offer Degree:

Chemical Engineering

University of Washington

Abstract

Zwitterionic Peptide Fusion Proteins for Therapeutic and Protective Applications

Patrick J. McMullen

Chair of the Supervisory Committee:
Shaoyi Jiang
Chemical Engineering

De novo design of peptide-based materials has become a common approach to introduce desirable properties into protein therapeutics. However, limited peptide-based technologies are capable of increasing the circulation time of and reducing the anti-drug antibodies (ADAs) of protein therapeutics as ADAs have been shown to reduce the circulation time and efficacy of many protein drugs following repeated administrations. Previous studies have shown the effective resistance of zwitterionic materials to non-specific protein adsorption. Zwitterionic materials such as polycarboxbetaine (pCB) are shown to be non-immunogenic. Glutamic acid (E) and lysine (K) containing zwitterionic peptides, which mimic protein surfaces, can be considered as the peptide

version of PCB polymers, and exhibit similar resistance to non-specific protein adsorption. Here we develop a novel zwitterionic peptide fusion protein platform for therapeutic applications. This unique peptide design with the zwitterionic EK motif takes into account the chemical, physical, and biological properties of the resulting peptides such as high hydration and increased hydrodynamic size. We show that these peptides have long circulation, low immunogenicity, and retained their circulation profiles for multiple injections. In addition, we scale up the production and purification of organophosphate hydrolase (OPH) and its PCB conjugate for improved protection against chemical warfare nerve agents.

ACKNOWLEDGEMENTS

The author would like to thank his advisor, Professor Shaoyi Jiang for support both monetarily and inspirationally for all the studies presented here. The author would also like to thank Dr. Zhefan Yuan, Dr. Caroline Tsao, Sijin Luozhong, Dr. Erik Liu, Dr. George Sellhorn, Haoxian Xu, Major Trevor Corrigan and all members in Prof. Jiang's research group for their kind help and insightful discussions. The author would especially thank his family for their support in this endeavor.

DEDICATION

This dissertation is dedicated to my mom and dad.

CHAPTER 1: INTRODUCTION

Arguably the immune response is the most prominent obstacle for therapeutics today. Numerous therapeutic tactics such as nanotherapeutics, *ex vivo* cell therapy, and protein drugs must all consider their interactions with the immune system (Baker, Reynolds, Lumicisi, & Bryson, 2010; De Almeida, Ransohoff, Nahid, & Wu, 2013; Fadeel, 2019; Schlosser et al., 2002). The mechanisms that govern the immune response to foreign materials have been the topics of extensive research for decades. The earliest studies focused on the body's response to foreign pathogens, resulting in the development of vaccines that have eradicated many diseases such as smallpox and limited the impact of many others such as measles, mumps, and the seasonal flu (Finco & Rappuoli, 2014). These innovations have utilized the physiological mechanisms to safely amplify the immune response to such pathogens, thereby, facilitating their elimination from the body. On the other hand, chemical moieties, such as tacrolimus and rapamycin, have more recently been implemented to suppress or hinder the over-activation of the immune system, which is the hallmarks of autoimmune diseases (Gummert, Ikonen, & Morris, 1999; Saunders, Metcalfe, & Nicholson, 2001). However, less progress has been made in the discovery of materials or moieties that exhibit low or no immune response and are thus deemed inert or non-immunogenic. Hence, the development of an innovative low immunogenic material technology is the focus of this dissertation.

As molecular interactions such as protein-protein interactions are necessary to trigger immunogenicity, natural mechanisms that block non-specific protein interactions were used as an initial design principle. In nature, proteins have evolved to prevent non-specific interactions to thwart protein aggregation in highly-dense protein environments to allow for normal physiological mechanisms to proceed. Fundamental studies to uncover these evolutionary patterns investigated

the amino acid frequency of residues exposed on the surface of over 1400 proteins in the blood serum and inside the cell as well as those residues on the interior of chaperone proteins, which function to fold and stabilize denatured proteins. It was found that negatively charged glutamic acid, E, and positively charged lysine, K, were most frequent and at equal ratios on the surface or interior of these proteins (White, Nowinski, et al., 2012)(White, Huang, & Jiang, 2012). Along the same line, various combinations of alternating charged amino acid sequences including the other charged amino acids aspartic acid (D) and arginine (R) were also tested for their adsorption of albumin, trypsinogen, and lysozyme, three abundant proteins in the body. In all these cases, the peptides containing E and K effectively resisted adsorption to these proteins, while peptides containing R performed significantly worse than those containing K (Chen, Cao, & Jiang, 2009; Nowinski, Sun, White, Keefe, & Jiang, 2012). Molecular dynamics studies examining arginine demonstrated that arginine more readily releases water compared to hydrated lysine, suggesting hydration or lack thereof plays an important role in these effects (White et al., 2013). Recent advances have further uncovered the tight water-binding properties of zwitterionic materials, which have proximal positive and negative charge domains (Hower et al., 2009). In nature, zwitterions, such as glycine betaine or trimethylamine-N-oxide, exhibit osmoregulatory function highlighting their unique affinity for water (Govrin, Tcherner, Obstbaum, & Sivan, 2018). For medical and biotherapeutic applications, polymeric zwitterions such as polycarboxybetaine (PCB) have performed exceptionally well. For example, PCB hydrogel implants resist capsule formation for up to 1 year and PCB protein conjugates exhibit no detectable accelerated blood clearance (ABC) following repeated injections (L. Zhang et al., 2013; P. Zhang et al., 2016, 2015). Capsule formation and the ABC effect are both the hallmarks of immunological responses against foreign materials together indicating that PCB is immunologically inert. Together, these promising results

point to the properties of high hydration and non-fouling as indicators of non-immunogenic materials, thus signifying that charge-alternating E and K may also be immunologically inert.

Current trends in biotechnology are shifting towards biologic drugs such as nucleic acids, proteins, lipids, and polysaccharides due to their compatibility with the body's metabolic processes. Protein drugs, in particular, have seen a great deal of success due to their specificity and potency (Leader, Baca, & Golan, 2008). Many of these require conjugation to a large polymer to maintain their favorable pharmacokinetic properties warranting difficult and inefficient conjugation procedures (Ishida & Kiwada, 2013). Therefore, a biocompatible polymer mimicking biologic would be particularly advantageous as a bioactive protein and a polymer-like peptide can be produced in one step by genetically fusing these two domains. In fact, this concept is already being pursued with the emerging technologies of XTEN and PAS (Podust et al., 2016; Schellenberger et al., 2009; Schlapschy et al., 2013). However, XTEN and PAS, as well as other technologies in pursuit, have not proved to be immunologically inert when fused to immunogenic proteins. Hence, a peptide sequence with low immunological reactivity is warranted as current technologies may face undesired immunogenicity. As E and K have opposing charges, we anticipate sequences with alternating charges to behave like other zwitterionic polymers such as PCB and prove to be immunologically inert. However, a fusion protein containing long EK sequences are expected to adopt structural tendencies that are not ideal for extended circulation times. Herein, we aim to design a non-immunogenic zwitterionic fusion protein encoding the alternating charged glutamic acid (E) and lysine (K) amino acids with structure disrupting amino acids for suitable biophysical characteristics for long circulation.

In chapter 2, we assess structural propensities in zwitterionic peptides that may be desirable in a peptide fused to a bioactive protein therapeutic. We show these structural tendencies

can be disrupted using random coil inducing amino acids. Then, we show that a zwitterionic peptide sequence with the structure-disrupting amino acid proline, termed EKP, fused to two therapeutic proteins, growth colony-stimulating factor (GCSF) and interferon alpha 2a, increase their circulation time in the body nearly seven-fold in mice and rats. As well, prolonged *in vivo* activity of GCSF is observed in rats demonstrating its benefits.

In chapter 3, we further explore zwitterionic peptide sequences to examine the effects of other structure-breaking amino acids on the *in vitro* and *in vivo* properties of zwitterionic peptides. Specifically, we examine the impact of proline, glycine, and serine content on the *in vitro* hydrodynamic size, stability, and bioactivity of zwitterionic peptides. As well, we probe their effects on circulation for one injection as well as their ability to maintain their pharmacokinetic profile after multiple injections. Finally, we correlate any reduction in circulation time after multiple injections to their immunogenicity.

In chapter 4, we probe the trends in the immunogenicity of zwitterionic peptides by conducting epitope mapping and alanine scanning experiments to determine the molecular drivers in the immunogenicity of zwitterionic peptides. Based on these results, we designed an EKX positional (i+1 to i+4) and rotational (P, S, & G) matrix and conjugated these peptides to KLH, a highly immunogenic carrier protein, and injected these into mice to aggressively screen for immune responses. The objective of these experiments was to observe the trends of EKX immunogenicity and develop non-immunogenic zwitterionic peptides for future applications.

In chapter 5, we develop a scaled-up expression and purification method for organophosphate hydrolase (OPH) and its high-density pCB-OPH conjugate to improve chemical and biological protection against nerve agents. Protection against nerve agents requires bacterially

derived OPH to achieve the rapid breakdown of these toxins. However, OPH is highly immunogenic with many exposed hydrophobic domains that require stringent protection using non-immunogenic polymers, such as zwitterionic polycarboxybetaine (PCB). Herein, we achieve this by a scaled-up expression and purification strategy to obtain sufficient quantities of well-protected PCB conjugated OPH.

CHAPTER 2: ZWITTERIONIC PEPTIDE FUSION PROTEINS EXHIBIT PROLONGED CIRCULATION TIME

INTRODUCTION

The design of long-lasting molecules in the body has been of considerable interest for many years for biotherapeutics applications, in particular for use in protein therapeutics. Many approaches have been developed to achieve this goal such as the use of polymers for nanoparticle formulation and conjugation, covalent linkage to lipids or carbohydrate moieties, as well as fusion of these to bioactive proteins such as fragment crystallizable region (Fc) and human serum albumin (HSA)(Strohl, 2015; Zhao et al., 2008). The most common approach to date is by conjugation to polyethylene glycol (PEG), which has shown clinical success with 14 FDA approved PEGylated drugs (Turecek, Bossard, Schoetens, & Ivens, 2016; Werle & Bernkop-Schnürch, 2006). Even so, alternatives such as genetic fusion to Fc and HSA have received much attention as well due to their ease of production, which does not require chemical conjugation. Fc and HSA, despite their attention and limited success, suffer from serious drawbacks such as instability and unwanted immunogenicity (Levin, Golding, Strome, & Sauna, 2015; M. M. Schmidt et al., 2013). Their instability and immunogenicity are suspected to be caused by improper folding during the production process resulting in exposure of protein domains leading to aggregation and exposure of immunogenic epitopes (Cromwell, Hilario, & Jacobson, 2006; Rosenberg, 2006; Sharma, 2007). To circumvent these limitations, the de novo design of random coil peptides has come forth as alternatives.

To date, the most well-known random coil peptides designed to increase the circulation time of protein therapeutics are XTENylation and PASylation. XTEN's technology is comprised of a random sequence with fixed ratios of proline (P), alanine (A), serine (S), threonine (T), glycine (G), and glutamic acid (E) (Podust et al., 2016; Schellenberger et al., 2009). As of 2016, XTEN

has been shown to be effective at extending the half-life of exenatide, glucagon-like peptide-2 , hGH, glucagon, Factor VIIa, Factor VIII, Factor IX as well as others (Podust et al., 2016). As of 2017, Bioverativ received acceptance of Investigational New Drug Application for BIVV001 for hemophilia treatment. BIVV001 is a recombinant Factor XIII Fc Von Willebrand Factor XTEN fusion protein. The drug is a novel once weekly treatment for hemophilia a (T. Lissitchkov, D. Rudin, J. Fruebis, K. Rice, S. Poloskey, L. Frohlich, S. Katragadda, 2019). XTEN contains a negatively charged glutamic acid which resists cell binding by repulsive mechanisms as cell membranes also exhibit a partial negative charge (Podust et al., 2016). The biodistribution of XTEN is limited to the bloodstream and cannot penetrate deep into tissues. As a result, BIVV001 requires Fc to facilitate transcytosis and escape from blood vessels into the extracellular matrix of tissues.

Alternatively, PAS was inspired by evolved peptide linkers. Proteins often contain two domains separated by a peptide linker to prevent the two domains from interacting or to control their interaction (Reddy Chichili, Kumar, & Sivaraman, 2013). These linkers are often composed of flexible repeats of glycine (G) and serine (S), which are thought to behave like polymers such as polyethylene glycol (PEG). However, repeats of G and S actually yielded poorer half-life extension compared to PEG, which was attributed to a peptide sequence that was too flexible causing the collapse of the peptide (Schlapschy et al., 2007). Proline (P) and alanine (A) were selected to replace glycine (G) in their original design (Schlapschy et al., 2013). Proline functions to stiffen the peptide as it forms a unique imide bond as opposed to the typical amide bond of all other amino acids, thus, preventing the collapse of the peptide observed with the glycine variants. Similarly, alanine is used as its one carbon side chain will reduce rotation along the peptide backbone and, therefore, counteract the collapse of the peptide. Homopolymers of P and A are

known to form the secondary structures PPII helix and alpha helix respectively (Schimmel & Flory, 1968). However, mixtures of P and A disrupt the secondary structures of the respective homopolymer forming a random coil, which again would mimic polymer behavior (Schlapschy et al., 2013). Still, the high proline and alanine are likely to make the peptide hydrophobic introducing potential immunogenicity in future trials.

Learning from these designs, we recognize the importance of preventing secondary structure formation for the design of zwitterionic peptide fusion proteins. Based on the peptide theory put forth by Flory and co-workers, amino acids with side chains, such as glutamic acid and lysine, tend to form secondary structures (Brant, Miller, & Flory, 1967; SCHIMMEL & FLORY, 1967). Therefore, we examined the secondary structure properties of short 30 amino acid EK peptides by circular dichroism. Then we design EK peptides with proline (termed EKP) to disrupt secondary structure formation and extend the peptide conformation to prevent collapse and increase the circulation time of growth colony-stimulating factor (GCSF). GCSF is commonly used to treat neutropenia following chemotherapy in cancer patients and requires multiple injections due to short circulation time (Molineux, 2005; Scholz et al., 2009). We produce EKP fused to GCSF (EKP-GCSF) in *E. coli* and demonstrate its extended circulation time compared to GCSF in mice and rats manifesting into elevated white blood cell counts for extended times following injection in rats suggesting prolonged efficacy. In addition, we also demonstrate prolonged circulation with EKP fused interferon alpha 2a (IFN), another protein therapeutic with short circulation time used to treat hepatitis c as well as hairy cell leukemia (Matthews & McCoy, 2004; Okanny et al., 2000).

METHODS

Protein Expression of GCSF and EKX-GCSF in E. coli

For EKX-GCSF expression, pMALc5E vectors containing EKX-GCSF sequences were transformed into BL21 (DE3) *E. coli*. 10 mL Lysogeny Broth (LB) with 100 µg/mL ampicillin starter cultures were incubated overnight at 37ºC and transferred to 500 mL Terrific Broth (TB) with 100 µg/mL ampicillin. Cultures were grown at 37ºC until OD600 of .5, at which point expression was induced with 1 mM Isopropyl-β-D-thiogalactoside (IPTG). Then, cultures were shifted to 30 ºC for 6 hrs at which point they were harvested by centrifugation and frozen at -80 ºC until purification.

For GCSF expression, pET20b+ vectors containing the GCSF sequence were transformed into BL21 (DE3) *E. coli*. 20 mL LB with 100 µg/mL ampicillin starter cultures were incubated overnight at 37ºC and transferred to 1L TB with 100 µg/mL ampicillin. Cultures were grown at 37ºC until OD600 of .5, at which point expression was induced with 1 mM Isopropyl-β-D-thiogalactoside (IPTG). Cultures were then grown for 24 hrs post induction at 37ºC at which point they were harvested by centrifugation and frozen at -80 ºC until purification.

EKP-GCSF Purification, Folding, and Cleavage of MBP tag

For EKP-GCSF, pellets were resuspended in 20 mL of 20mM sodium phosphate, 6M guanidine hydrochloride (GnHCl), 10 mM imidazole, 500 mM NaCl, and 1 mM phenylmethylsulfonyl fluoride pH 8. Resuspended pellets were lysed using a probe sonicator (50% amplitude 10 seconds on 30 seconds off for 20 minutes) and clarified by centrifugation. The supernatant was then precipitated in 80% ethanol pelleted by centrifugation to get rid of lipids. Then, the pellet containing precipitated proteins was resuspended in 20 mL of the same buffer

without PMSF. The resulting solution was applied to a 5mL BioScale Mini Nuvia Ni-Charged IMAC column. The column was washed using a decreasing pH gradient from 8 to 4. MBP-EKX-GCSF-HIS was eluted off the column at pH 4.

At this point the protein was dialyzed against the following refolding buffer for 12 hour periods. Any precipitated protein was removed by centrifugation. 10 mM DTT was added to the eluate and it was dialyzed against 2M GnHCl, 50 mM Tris, pH8 (fold buffer 1). Fold buffer 2: 1M GnHCl, 400mM L-arginine, 50 mM Tris, 1mM oxidized glutathiones, and 2mM reduced glutathiones pH 8; Fold buffer 3: 500mM GnHCl, 400mM L-arginine, 50 mM Tris, 1mM oxidized glutathiones, and 2mM reduced glutathiones pH 8. Fold buffer 4: 100 mM L-arginine, 50 mM Tris, 250 mM NaCl, 1 mM oxidized glutathiones, 2 mM reduced glutathiones pH 8. Fold Buffer 5: 50 mM Tris 50 mM NaCl pH8.

Then, the proteins were concentrated to about 500 uL (5-10 mg/mL), and 2mM CaCl2 was added. 160 units of enterokinase were added to MBP-EKP-GCSF-HIS proteins for removal of the MBP. The cleavage reaction was done at 20 ^{o}C for 16 hr and terminated with 1mM PMSF. Subsequently, the EKP-GCSF-HIS was separated from MBP and enterokinase using size exclusion chromatography (SEC- Enrich SEC 70 Biorad).

GCSF Purification and Folding

For GCSF, pellets were resuspended in 60 mL phosphate buffered saline (PBS) with 1mM PMSF. Resuspended pellets were lysed using a probe sonicator (50% amplitude 10 seconds on 30 seconds off for 20 minutes) and centrifuged for inclusion body isolation. Pellets were retained and washed 2 times with 20 mM Tris 5mM EDTA .5% Triton X-100 pH8. Pellets were then resuspended in 6M GnHCl 50 mM 10 mM DTT pH 8. Folding was subsequently conducted as

with EKP-GCSF. GCSF was then dialyzed against 50 mM glycine 25 mM NaCl pH 5.5 to precipitate contaminants. The resulting solution was then applied to a 5 mL cation exchange column (CaptoS ImpRes GE) and eluted with a gradient from 25 mM to 1M NaCl. Fractions containing GCSF were pooled and applied to an SEC column in PBS for cleanup.

Circular Dichroism

EKX-GCSF and GCSF diluted to 1 μM in 10 mM Potassium Phosphate buffer pH 8. Circular dichroism spectra were obtained Jasco 720 CD spectrophotometer using a .1 cm thickness quartz cuvette. Spectra were smoothed using the Jasco smoothing software. To obtain the CD spectra for the EKX domain, the CD spectra from GCSF was subtracted from that of EKX-GCSF.

EKP-IFN Gene and Plasmid Design

DNA sequences encoding interferon alpha-2-a (IFN), EK, and EKP were synthesized by Genscript. A hemagluttanin (HA) tag was appended to the N-terminal of IFN. 30 kDa EK and EKP sequences were inserted between the HA tag and IFN. A trans-plasminogen (tPA) activator secretion tag was inserted on N terminus of the constructs for secretion into the media. All sequences were optimized for mammalian cell expression and inserted into pcDNA3.1+ plasmids with a Kozak sequencer and CMV promoter for constitutive expression.

Plasmid Preparation

Plasmids encoding HA-IFN and HA-EKP-IFN were transformed into DH10B *E. coli*. Starter cultures were grown for 8 hours with TB/amp at 37C. Then, they were transferred to 150 mL of LB/amp and incubated overnight at 37C. Plasmids were extracted from the cultures using ZymoPURE II Maxiprep Kit according to the manufacturer's instructions.

Transfection into HEK293F mammalian cell cultures and purification

Plasmids were transfected into HEK293F cells cultured in FreeStyle Media at 37C and 5% CO2. Transfection was carried out in 30 mL cultures at $1x10^6$ cells/mL. 180 μg Polyethylimine (PEI) and 30 μg plasmids were complexed for 15 minutes in 1 mL of media and added to cells. Expressions were carried out for 72 hours and the media harvested for expressed protein. Protein was purified by Pierce HA tag IP/Co-IP Kit (Thermo Fisher) according to the manufacturer's instructions.

Differential Scanning Calorimetry

5 μL of 12.5X SYPRO Orange (Invitrogen) was mixed with 20 μL of HA-EKX-IFN or HA-IFN at a concentration of 0.5 mg/mL. Relative fluorescence units were measured using the Bio-Rad CFX RT-PCR machine. Temperatures were increased from 10°C to 90°C with 0.5°C, 1 minute intervals.

EKX-IFN Activity Assay

The activity of EKX-IFN and IFN was determined by the inhibition of proliferation of Daudi B cells. Various concentrations of protein were incubated with 5x10^4 cells per well of Daudi B cells in a 96 well plate. Equimolar concentrations were compared between EKX-IFN and IFN. These were incubated for 72 hours and proliferation was measured by CellTiter 96 Aqueous One solution with 20 μL per well. The reagent was incubated for 4 hours and absorbance was measured at 592 nm. Percent viability was calculated using no cells and no protein controls.

Pharmacokinetics in mice

Adult C57BL/6 mice were injected retro-orbitally with EKP-GCSF at 1 mg/kg and GCSF at .4 mg/kg. Blood was drawn at the indicated time points by chin bleed and serum was isolated by centrifugation. Serum concentrations of GCSF and EKP-GCSF were determined by capture ELISA.

Enzyme Linked Immunosorbent Assay of GCSF and EKP-GCSF

High binding EIA/RIA ELISA plates were coated with 1:1000 dilution of monoclonal anti-GCSF antibody (ThermoFisher) in sodium bicarbonate buffer overnight at 4 degrees Celsius. Wells were washed with PBS + 0.03% Tween and blocked with 3% BSA+PBS+0.03% Tween (blocking buffer) at 37degrees C for 2 hrs. 3 μL serum was diluted in 100 μL of blocking buffer and incubated at 37 degrees C for 2 hr. Wells were washed and incubated with 1:5000 (EKP-GCSF) or 1:10000 (GCSF) polyclonal anti-GCSF primary antibody (R&D systems) in blocking buffer for 1.5 hours at 37 degrees C. Plates were washed and incubated with 1:10000 anti-goat HRP secondary antibody in blocking buffer at 37 degrees C for 1 hour. These conditions were the same for both the mice and rat studies.

Enzyme Linked Immunosorbent Assay of HA-IFN and HA-EKP-IFN

High binding EIA/RIA ELISA plates were coated with 1:1000 dilution of monoclonal anti-HA antibody (Novus) in sodium bicarbonate buffer overnight at 4 degrees Celsius. Wells were washed with PBS + 0.03% Tween and blocked with 3% BSA+PBS+0.03% Tween (blocking buffer) at 37degrees C for 2 hrs. 5 μL serum was diluted in 100 μL of blocking buffer and incubated at 37 degrees C for 2 hr. Wells were washed and incubated with 1:5000 polyclonal anti-IFN primary antibody (MyBioSource) in blocking buffer for 1.5 hours at 37 degrees C. Plates were

washed and incubated with 1:10000 anti-rabbit HRP secondary antibody in blocking buffer at 37 degrees C for 1 hour.

Pharmacokinetics and Pharmacodynamics in rats

Sprague Dawley rats were injected by tail vein injection with EKP-GCSF at .5 mg/kg and GCSF at .2 mg/kg. Blood was drawn at the indicated time points from the tail vein, and serum was isolated by centrifugation. Serum concentrations of GCSF and EKP-GCSF were determined by capture ELISA.

Sprague Dawley rats were injected under the same conditions as the pharmacokinetics study. Blood was drawn every 24 hrs from the tail vein and 1 mM EDTA was added. White blood cell counts were determined using Leuko-TIC 1:20 white blood cell count kit according to the manufactures' instructions.

RESULTS AND DISCUSSION

Previous work from Nowinski *et al.* demonstrated that a short 7 amino acid EK sequence exhibits a random coil according to circular dichroism analysis (Nowinski et al., 2012). This is consistent with the hydrophobic effect, which suggests such a hydrophilic peptide, lacks a driving force for protein folding (Dobson, Šali, & Karplus, 1998). However, simulations of longer 30 amino acid EK sequences by Dr. Joshua Smith suggested that salt bridges could potentially stabilize a β twist type secondary structure, but were disrupted by the insertion of glycine residues interspersed in the sequence (Smith, McMullen, Yuan, Pfaendtner, & Jiang, 2020). These structural tendencies seen in simulations were also prevalent in experimental circular dichroism analysis of 30 amino acid EK peptides and 28 amino acid EKGG peptides.

The β sheet structure of EK observed with these data are of particular importance for the design of long-circulating peptides. Specifically, random coil peptides are expected to have an increased radius of gyration compared to those forming stable structures, which is typically associated with reduced renal clearance and prolonged retention in the body (Dutta & Bhattacharyya, 2001; Molineux, 2005; Wang, Plaxco, & Makarov, 2007). Therefore, zwitterionic peptides will benefit from structure-breaking residues to increase the radius of gyration .

Informed by previous structure studies, EK peptide sequences were designed with the amino acid proline (P) to disrupt potential secondary structure with EK and extend its conformation. Sequences were designed to minimize the repetitive moieties as we suspected repetition may have a negative impact on the expression of the peptide, which was of considerable concern given the previously observed low expression with EK peptides (Figure 2-1). As the bioactive moiety and protein therapeutic domain, granulocyte colony-stimulating factor (GCSF)

was selected because GCSF requires PEGylation to prevent its rapid clearance (Arvedson, O'Kelly, & Yang, 2015; Molineux, 2005). Moreover, the most commonly marketed version of PEG-GCSF, Neulasta, consists of a 20kDa linear PEG chain conjugated to the N-terminus of GCSF suggesting a N-terminally linked fusion protein will at least perform comparably to Neulasta (Strohl, 2015).

Initially, attempts to express EKP-GCSF without a fusion partner were unsuccessful. Therefore, maltose-binding protein (MBP) was appended to the N-terminus of the protein with an enterokinase cleavage site for later removal (Figure 2-2a). The MBP fusion constructs significantly improved the expression of the protein due to its strong expression and improved solubility. Initially, we tried to purify MBP-EKP-GCSF using amylose resin, which binds to the MBP domain and can be eluted easily using maltose. However, the MBP domain did not bind well to the amylose column potentially due to the non-fouling properties of EKP. Therefore, we added a 6x HIS tag to the C-terminus of the protein as an alternative (Figure 2-1a). In order to expose the HIS tag for binding to an IMAC column, we denatured the protein with both 6M guanidine hydrochloride, which significantly improved its affinity (Figure 2-1a). To refold, a modified protocol was adopted from Thomson, Olson, Jackson, & Schrader, 2012. Briefly, following elution, 10mM DTT was added to the eluate to reduce improperly formed disulfide bonds, and the resulting solution was transferred to snakeskin tubing for stepwise dialysis. All dialysis steps were buffered in 50 mM Tris pH8 and proceed with the following steps: 2 M GnHCl to 1M GnHCl, 0.4 M Arginine, 3 mM glutationes 2:1 reduced:oxidized to 0.1 M Arginine, 250 mM NaCl, 3 mM glutationes 2:1 reduced:oxidized to 50 mM NaCl (Figure 2-1a). Protein solution was centrifuged in between steps to remove precipitated protein. Other protocols were tried to refold but were unsuccessful due to excessive precipitation of the product.

Following folding, removal of the MBP was performed using enterokinase. The efficiency of enterokinase cleavage was greatly enhanced by reducing the reaction volume. However, some uncleaved protein remained. The remaining uncleaved protein as well as MBP and enterokinase were removed by size exclusion chromatography (Figure 2-1a). Primarily one band is visible by SDS-PAGE analysis indicating EKP-GCSF-HIS was purified (Figure 2-2a). Mass spectrometry showed a molecular weight of 52129 kDa indicating the correct protein is being produced. EKP-GCSF was further characterized by examining the structure of circular dichroism compared to the unfused GCSF. The CD profile of GCSF clearly shows a two minimum at 222 nm and 208 nm indicating the presence of alpha helices, which is consistent with the known structure of GCSF (Figure 2-2d) (Brems, 2008) . The EKP-GCSF shows a faint minimum near 222 nm suggesting the formation of alpha helices as expected for GCSF and a much stronger minimum near 205 nm (Figure 2-2d). This could be due to the formation of a PPII helix structure, which typically demonstrates a minimum near 205 nm (Woody, 2010). Subtraction of the GCSF circular dichroism spectra from that of EKP-GCSF also showed a minimum near 195 nm suggesting EKP adopts random coil conformation (Figure 2-2e). In addition, EKP-GCSF was shown to elute at a much larger hydrodynamic radius compared to bare GCSF by size exclusion chromatography (SEC) analysis (Figure 2-2c). Interestingly, SEC also revealed multiple smaller peaks that elute earlier than the main GCSF peak, which could indicate that GCSF is exhibiting aggregation behavior in vitro, which has been reported before with GCSF (Figure 2-2c).

Given the difficulty of producing zwitterionic peptides in *E. coli*, we explored mammalian cell expression systems to evaluate their expression behavior of zwitterionic peptides. We selected interferon alpha 2 a (IFN) as another model protein needing PEGylation to increase its circulation time *in vivo*. For the mammalian specific mammalian cell system, HEK293F cells were used as

they are typically used for overexpression of proteins needing modification only easily achievable using eukaryotic systems such as glycosylation (Figure 2-1b). Moreover, as suspension cells, increased oxygenation by shaking allows for increased expression yields, which is likely a necessity for zwitterionic peptides. We inserted a transplasminogen activator secretory sequence upstream of the IFN gene to secrete the product into the media and an hemaglutanin tag enabling a highly specific one-step purification (Figure 2-1b). Strong expression was observed with this design for EKP-IFN and one-step purifications were successful at achieving a uniform product as visible by SDS-PAGE (Figure 2-3a). Purification yields were typically around 100 μg per 30 mL culture of HEK293F cells transfected with EKP-IFN encoding plasmid, which was similarly observed with IFN alone suggesting EKP does not inhibit protein expression in mammalian cells observed in *E. coli*.

EKP-IFN also showed significantly larger hydrodynamic size compared to the unfused counterpart as demonstrated by size exclusion chromatography (SEC) (Figure 2-3b). Moreover, differential scanning calorimetry revealed a higher thermal melting temperature of 56.7 degrees Celsius for EKP-IFN compared to 53.5 degrees Celsius for IFN (Figure 2-3c). EKP peptide alone did not show any thermal shifting behavior due to its random coil conformation (data not shown). Thus, EKP likely improves the thermal stability of IFN similar to EK-ß lactamase (Liu et al., 2015).

To investigate the functionality of EKP-IFN, we examined the anti-proliferative activity of EKP-IFN on Daudi B cells as IFN prohibits the proliferation of Daudi B cells *in vitro* by binding to the type I IFN receptor present on the cell membrane. The anti-proliferative activity of EKP-IFN is reduced compared to IFN alone, with the EC50 increasing from 2.00 +/- 0.24 nmol/μL for unfused IFN to 193 +/- 28 nmol/μL for EKP-IFN. The decrease in activity may be related to IFN

as PEG-IFN and HSA-IFN fusions have notoriously low *in vitro* activity (Bailon et al., 2001; Zhao et al., 2008). As IFN is a receptor-binding protein, steric mechanisms are contributing to reduced activity. A flexible linker between the IFN and EKP domains would abrogate the activity loss.

In order to examine the pharmacokinetic properties of EKP peptides, we retro-orbitally injected adult C57BL/6 mice with 1 mg/kg EKP-GCSF and HA-EKP-IFN as well as their unfused counterparts and drew blood at several intervals post injection. We examined the serum concentration at the indicated time points using a capture ELISA. The capture ELISA was significantly less sensitive for both the EKP-GCSF and HA-EKP-IFN compared to the unfused counterparts, thus demonstrating the non-fouling ability of zwitterionic peptides (data not shown). EKP fusions have clear half-life extension properties compared to the unfused GCSF or IFN. The serum concentration of the unfused proteins decreased rapidly after injection, while the serum concentration of the EKP variants was maintained at significantly higher concentrations after injection as both EKP-GCSF and EKP-IFN were detectable for 8 hours post injection (Figure 2-4a & b). The circulation half-life of EKP-IFN was approximately 6.9 times greater than IFN alone with half-lives of 2.55 +/- 0.38 hrs and 0.37 hrs +/- 0.02 hrs respectively (Table 2-1). The fold increase for EKP-GCSF compared to GCSF alone was not calculable because the concentration of GCSF was below detection at the third collected time point. However, the half-life of EKP-GCSF was 3.43 +/- 0.20 hrs, which is comparably longer than EKP-IFN. (Table 2-1) Therefore, we chose to proceed to test EKP-GCSF with rats.

In rats, we observed a 6.1 fold circulation half-life increase with EKP-GCSF compared to the unfused protein, which is consistent with our previous results in mice (Figure 2-4c). Furthermore, we examined the white blood cell counts in rats for 72 hours post injection. GCSF induced an increase in white blood cell counts 24 hours post injection, which was no longer present

at 48 hours and 72 hours (Figure 2-4d). However, EKP-GCSF maintained increased white blood cell counts for up to 72 hours indicating that it has prolonged activity *in vivo* (Figure 2-4d). The area under the curve (AUC) values for the WBC count post injection were 5.7 +/- 3.4 & 5.3 +/- 0.8 hr*cells/mL for GCSF and EKP-GCSF respectfully. Together, these data suggest that any potential decrease in receptor binding with the GCSF receptor is compensated by the increased circulation time, which is consistent with PEG-GCSF studies that exhibited an inverse relationship between *in vitro* activity and *in vivo* activity (FISHBURN, 2008). Overall, EKP-GCSF is a potential replacement for PEG conjugated GCSF as it demonstrates both prolonged circulation and high activity *in vivo*.

CONCLUSIONS

Herein, EK peptides were shown form a partial β sheet structure that is eliminated by glycine. As stable structures are not desirable for peptides that extend the circulation time of therapeutic proteins, we sought to abrogate the β sheet structure observed in EK peptides with structure breaking amino acid proline. MBP-EKP-GCSF was shown to be expressed and purified from *E. coli*. We also refold EKP-GCSF *in vitro,* suggesting EKP does not interfere with the folding of GCSF. Demonstrating the versatility of the EKP sequence, we explore EKP-IFN expression in HEK293F mammalian cells and demonstrate that EKP-IFN is stably expressed in HEK293F. Then, the pharmacokinetics and pharmacodynamics of EKP fusion proteins were studied *in vivo*. We show EKP increases the circulation time of both GCSF and IFN in mice compared to their unconjugated counterparts. We also show EKP improves the circulation of GCSF in rats thereby indicating that the improved circulation due to EKP is robust and obvious in multiple systems. Furthermore, we examine the *in vivo* activity of EKP-GCSF in rats and show that the enhanced circulation prolongs the *in vivo* activity of GCSF. These results have potential implications to improve the treatment of neutropenia post-chemotherapy with the possibility of replacing PEG.

FIGURES AND TABLES

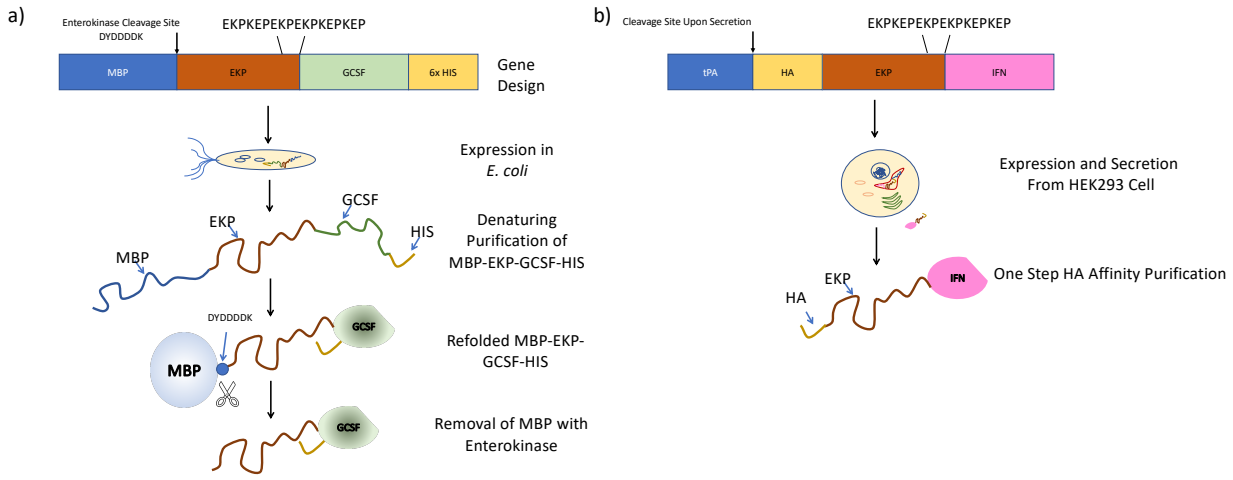

Figure 2-1: Gene design, expression, and purification strategy for (a) EKP-GCSF expressed in *E. coli* and (b) EKP-IFN expressed in HEK293F mammalian cells.

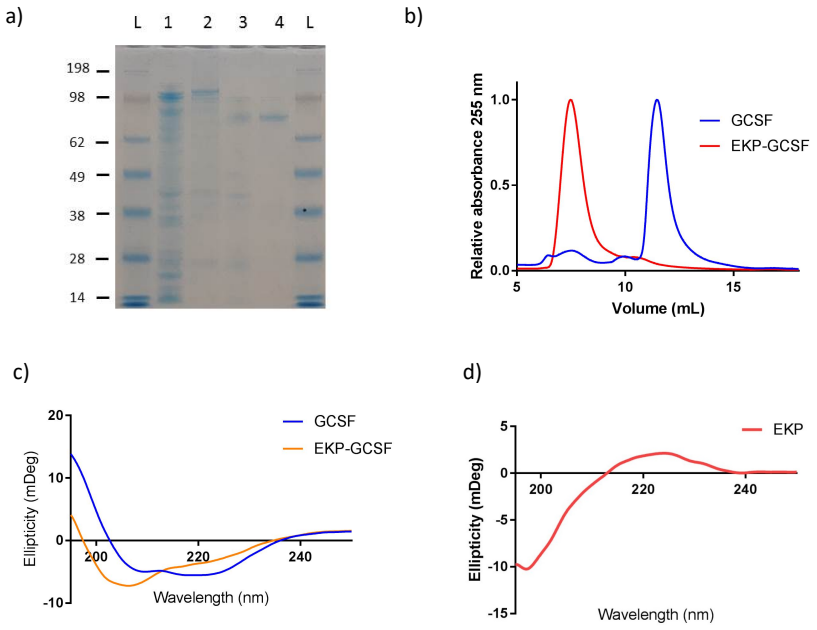

Figure 2-2: Purification and biophysical characterization of EKP-GCSF from *E. coli*. (a) SDS-PAGE analysis of EKP-GCSF purification from *E. coli* cell lysate. Molecular weight ladder is from SeeBluePlus 2 standard. Lane 1: 6 hours post induction cell lysate, Lane 2: Eluate from IMAC column. Lane 3: Product following folding and enterokinase cleavage. Lane 4: Product following size exclusion chromatography. (b) Size Exclusion Chromatography (SEC) Analysis of EKP-GCSF and GCSF. This was done using BioRad Enrich SEC 70. (c) Circular dichroism spectra of GCSF and EKP-GCSF diluted to 1 µM in 10 mM Potassium Phosphate buffer pH 8. (d) EKP circular dichroism spectra obtained by subtracting GCSF spectra from EKP-GCSF spectra.

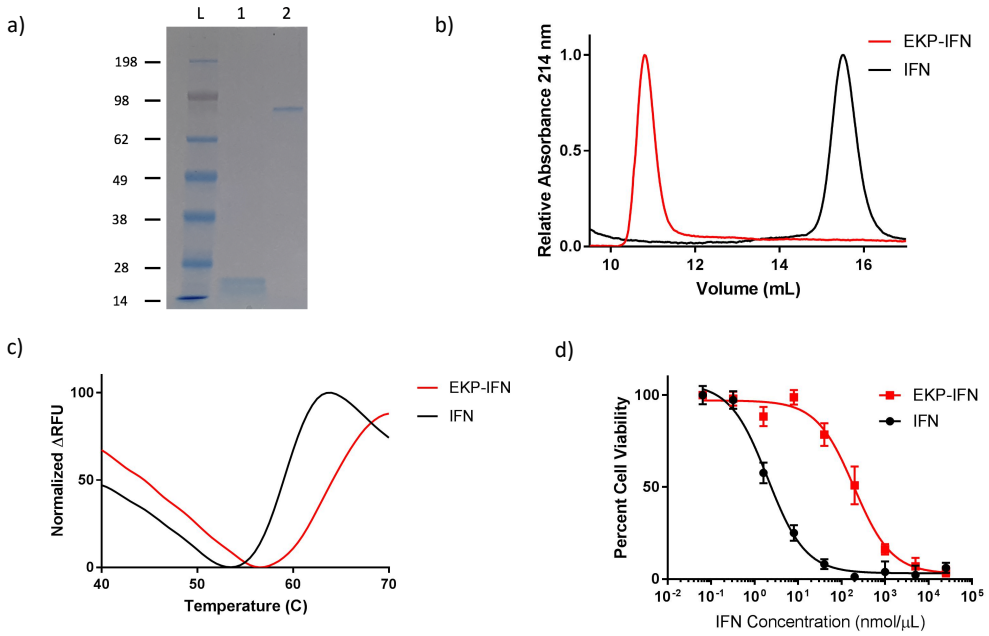

Figure 2-3: Purification and characterization of EKP-IFN (a) SDS-PAGE gel of purified HA-IFN (lane 1) and HA-EKP-IFN (lane 2). (b) Size exclusion chromatography of EKP-IFN and IFN. (c) Differential scanning calorimetry detected by change in relative fluorescence units exposed to a temperature gradient for IFN and EKP-IFN incubated with SYPRO Orange. (d) Anti-proliferative activity of IFN and EKP-IFN on Daudi B cells.

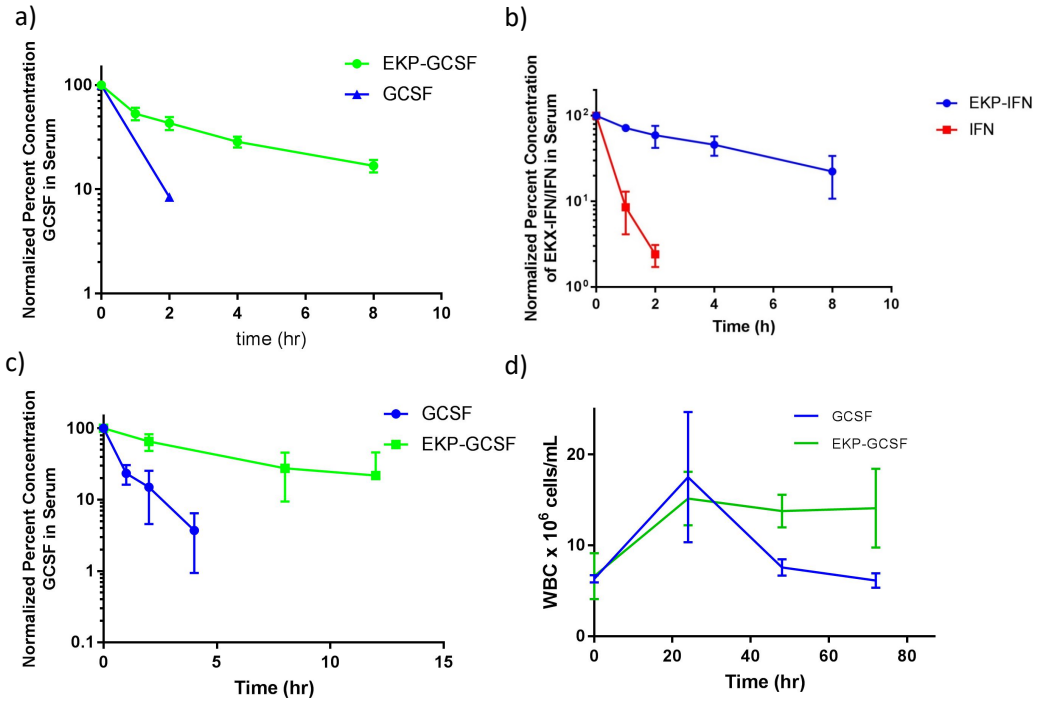

Figure 2-4: Intravenous pharmacokinetics of EKP-GCSF and GCSF in (a) C57BL/6 mice and (c) Sprague Dawley rats. (b) Intravenous pharmacokinetics of EKP-IFN and IFN in C57BL/6 mice. (d) White blood cell count following intravenous injection of EKP-GCSF and GCSF in Sprague Dawley rats.

Injected Protein	Recipient Animal	I.V. Half-life (hrs)
GCSF	Sprague Dawley Rat	0.89 +/- 0.22
EKP-GCSF	Sprague Dawley Rat	5.42 +/- 0.42
GCSF	C56BL/6 Mice	-
EKP-GCSF	C56BL/6 Mice	3.43 +/- 0.20
IFN	C56BL/6 Mice	0.37 +/- 0.02
EKP-IFN	C56BL/6 Mice	2.55 +/- 0.38

Table 2-1: Intravenous circulation half-life for EKP-GCSF and GCSF injected in rats and mice. Intravenous circulation half-life for IFN and EKP-IFN injected into mice.

CHAPTER 3: ZWITTERIONIC PEPTIDE FUSION PROTEINS SHOW LOW IMMUNOGENICITY AND RETAINED CIRCULATION TIME

INTRODUCTION

Protein drugs are promising therapeutic tools, as through evolution and improvements attainable by molecular biology, they have high potency and specificity compared to other therapeutics (Sauna et al., 2017). However, they are rapidly cleared from the circulation and, thus, require frequent injection to maintain therapeutically effective concentrations in the body (Werle & Bernkop-Schnürch, 2006). PEGylation is the gold standard modification method for protein drugs to reduce the required injection frequency as it increases the radius of hydration and gyration of the molecule and protects it from undesirable interactions such as hepatic uptake, renal clearance, and immunological responses (Swierczewska, Lee, & Lee, 2015; Webber et al., 2016; Werle & Bernkop-Schnürch, 2006). Even so, in recent years, the potential immunogenicity of PEG has called into question its effectiveness as several protein drugs have been shown to induce anti-PEG antibody production (Ishida & Kiwada, 2013; Li et al., 2018; Qi Yang, 2015). For example, PEG conjugated to uricase, which is marketed as the drug PEGloticase and used to treat gout, exhibited antibodies in 89% of patients, with 60% of these patients becoming non-responsive to the drug likely due to the anti-PEG antibodies (Sundy et al., 2011). In addition, as PEG is frequently used in cosmetic products, estimates as high as 72% of the population are suspected to already have anti-PEG antibodies, which could lead to a significant loss in efficacy and even anaphylaxis to many more PEGylated therapeutics (Yang et al., 2016). The potential induction of anti-PEG antibodies and prevalence of pre-existing anti-PEG antibodies poses a serious risk as they may reduce the circulation half-life of the protein drug by the accelerated blood clearance (ABC) effect or provoke an even more severe anaphylactic response. Therefore, protein drug

modification methods to increase the circulation time in the body demand non-immunogenic alternatives.

The immune reactions to PEG raise the question of what is triggering PEG recognition by the immune system and how can we learn from the shortcomings of PEG to engineer peptides that will not be recognized by the immune system. Previous work in our group studied the mechanisms on the resistance of PEG to non-specific protein interactions when coated on surfaces (Zheng, Li, Chen, & Jiang, 2004). Studies from our group demonstrated that although chain flexibility does indeed play a role in the anti-fouling mechanism, the role of hydration was largely overlooked. Moreover, when comparing densely packed self-assembled monolayers (SAMs) of oligoethylene glycol (OEG) with densely packed SAMs containing mixed charged polymers, the tightly packed SAMs with mixed charged polymers performed significantly better in resisting non-specific protein adsorption due to the more tightly bound water molecules around the mixed charge polymers compared to OEG, thereby highlighting the significance of hydration in resisting non-specific protein adsorption (Chen, Yu, Yu, He, & Jiang, 2006). Applying these concepts to zwitterionic peptides, flexible and highly hydrated zwitterionic peptides ought to be less immunogenic due to the combined effects of increased peptide flexibility and increased hydration from zwitterionic moieties.

Alternatively, as a significant body of data already exists regarding peptide immunogenicity and as methods to predict immunogenic sequences versus non-immunogenic sequences are actually quite plentiful, it may be possible to use these predictive tools to design non-immunogenic zwitterionic sequences. Broadly, they can be categorized into two types: B cell dependent/B cell receptor prediction methods and T cell-dependent/MHCII dependent prediction methods (Bryson, Jones, & Baker, 2010). T cell dependent prediction methods rely on sequence

dependent Major Histocompatibility Complex II (MHCII) propensities of peptide antigens. As MHCII is responsible for loading and presenting peptides to T cell receptors (TCRs), it is a critical regulator of peptide immunogenicity (O'Brien, Flower, & Feighery, 2008; Sant'Angelo, Robinson, Janeway, & Denzin, 2002). Following MHCII loading and binding to TCRs, naïve CD4+ T cells become activated triggering proliferation and differentiation into Th1 cells, Th2 cells, Th17 cells, or T reg cells. *In silico* prediction algorithms based on the loading propensity of peptides into MHCII DR, DP, and DQ, the peptide loading type of MHCII, and the various alleles have seen some success by revealing patterns in peptide binding such as critical P1 and P4 anchor residues (Nielsen, Lund, Buus, & Lundegaard, 2010). Broad correlations have suggested immunogenic T cell epitopes tend to be hydrophobic, thus, point to the importance of hydrophilicity in preventing immunogenicity (Chowell et al., 2015). However, many studies have seen poor predictive abilities of *in silico* trained models likely due to the complex biological factors necessary to trigger a T cell dependent immunogenic response (Flower, 2003; J. Schmidt et al., 2017).

BCR and B cell dependent prediction methods have also seen difficulty, but for different reasons. First, for BCR binding, the tertiary structure of the protein antigen must be considered as opposed to a linear peptide epitope. BCR binding sequences must be surface exposed providing a favorable interface for the BCR to bind with the antigen. As a matter of fact, initial BCR prediction models focused on protein shape. Peptide domains that protruded from the globular protein core were considered more likely to interface with the BCR (Ponomarenko et al., 2008). Moreover, given those surface residues of a protein tend to be hydrophilic due to protein folding energetics, hydrophilicity was considered to be a positive predictive identifier for BCR binding (Kolaskar & Tongaonkar, 1990). BCR binding prediction methods have seen some success, but are severely

limited due to the amount of structural information needed as an input to the model as opposed to only a primary amino acid sequence (Jespersen, Mahajan, Peters, Nielsen, & Marcatili, 2019).

In light of the uncertainty in predicting the non-immunogenic sequences, we recognized the importance of maintaining the flexibility of EK containing peptides as the flexibility of PEG was known to play a role in its non-fouling mechanism. The addition of more hydrophilic properties to a flexible peptide would prevent unwanted uptake by the liver, reduce renal clearance, and avert immune responses. Therefore, amino acids induce a random coil conformation of the peptide would maintain flexibility and abrogate any potential increase in antigenicity from integrating amino acids other than E and K. The most widely accepted amino acids that are known to induce random coil conformations are proline, P, and glycine, G (Schweitzer-Stenner, 2012; Swindells, Macarthur, & Thornton, n.d.). As well, serine is becoming more widely accepted as a random coil inducing amino acid due to its prevalence in protein linker domains (Sammond et al., 2012). However, these amino acids induce random coil conformations by three distinct mechanisms. Proline prevents hydrogen bonding of the peptide backbone due to its cyclic imine side chain, thus destabilizing alpha helices (Schimmel & Flory, 1967). In addition, proline restricts the rotational freedom of the peptide backbone, thus elongating the peptide and inducing a spheroid like peptide shape (Breibeck & Skerra, 2018). Glycine, on the other hand, increases the rotational freedom of the peptide backbone and prevents structure formation by entropic favoring of the random coil conformation (Imai & Mitaku, 2005; Schlapschy et al., 2007; Van Rosmalen, Krom, & Merkx, 2017). Serine, similar to glycine, has a short side chain and, thus, tolerates flexibility of the peptide backbone while maintaining favorable water interactions with the hydroxyl group on its side chain (Imai & Mitaku, 2005). To test the effects of these amino acids on the immunogenicity of zwitterionic peptides we designed three new sequences, EPKP, EKPS, and

EKPG, and compared their immunogenicity to EKP as a reference. EPKP was designed to have every other reside as proline to sample the effects of increasing the proline content which is expected to reduce the hydrophilicity and increase the radius of gyration. EKPG and EKPS replaced half of the proline residues from the EKP formulation with either glycine or serine respectively. These were selected to test the effects of replacing hydrophobic prolines with more hydrophilic glycine and serine residues, while simultaneously altering its structural properties.

To test these sequences, we selected IFN as the model fusion protein due to its activity in the blood as opposed to the activity in the bone marrow. In addition, the expression system we had established for IFN in HEK293F mammalian cells was significantly more suited for immunogenicity testing. Herein, we examine the immunogenicity of EKP and EKPX zwitterionic sequences to select for the zwitterionic peptide with the lowest immunogenicity.

MATERIALS AND METHODS

Plasmid Construction

All sequences were codon optimized for mammalian cell expression and synthesized by Genscript. The native secretion tag for interferon alpha 2 a (IFN) was replaced by a transplasminogen activator secretion tag. Upstream of the start codon, the Kozak consensus sequence (GCCACC) was included for improved expression. A hemaglutanin (HA) tag was inserted after the TPA secretion tag for detection and purification. For EKX containing sequences, EKX was inserted on the N-terminus of IFN with the HA tag on the N-terminus of EKX. These constructs were ligated into pcDNA3.1(+) with KpnI and ApaI cloning sites.

Plasmid preparation and expression

Plasmids were transformed into DH5α *E. coli*. Four colonies were cultured in 200 mL Terrific Broth (TB) overnight. Plasmids were isolated using PureLink HiPure Plasmid Maxiprep kit (ThermoFisher) yielding typically around 200 μg of DNA.

To express HA-EKX-IFN or HA-IFN, plasmids were complexed with polyethyimine (PEI) Max 40 kDa with a mass ratio of 3:1 PEI to DNA, which approximately 14:1 N/P. Complexes were transfected into Expi293F (Gibco) cultured in F17 expression media maintained at 37°C, 5% CO2, and 85% humidity. Cells were transfected at 1x10^6 cells/mL and cultured for 96 hours at which point media was harvested.

Protein Purification and Purity Analysis

Expression media was harvested and concentrated from 60 mL to 1 mL using Amicon Ultracentrifuge Concentrators. 100 μL of anti-HA conjugated agarose was incubated with the concentrated media for 4 hrs. The resin was then washed with 50 mM Tris-HCl, 50 mM NaCl,

0.05% Tween-20, pH 7.2. The bound protein was eluted using 100 mM glycine pH 2.7 and neutralized immediately using 1M Tris pH 9.

Purity was analyzed by SDS-PAGE run on 4-12% Bis/Tris Bolt gels and stained with No-Stain Protein Labeling Reagent (ThermoFisher). Also, samples were analyzed by size exclusion chromatography (SEC) using a Superdex 200 Increase 10/300 GL column with a 20 mL bed volume (GE Healthcare).

Differential Scanning Calorimetry

5 µL of 12.5X SYPRO Orange (Invitrogen) was mixed with 20 µL of HA-EKX-IFN or HA-IFN at a concentration of 0.5 mg/mL. Relative fluorescence units were measured using the Bio-Rad CFX RT-PCR machine. Temperatures were increased from 10°C to 90°C with 0.5°C, 1 minute intervals.

EKX-IFN Activity Assay

The activity of EKX-IFN and IFN was determined by inhibition of the proliferation of Daudi B cells. Various concentrations of protein were incubated with 5x10^4 cells per well of Daudi B cells in a 96 well plate. Equimolar concentrations were compared between EKX-IFN and IFN. These were incubated for 72 hours and proliferation was measured by CellTiter 96 Aqueous One solution with 20 µL per well. The reagent was incubated for 4 hours and absorbance was measured at 592 nm. Percent viability was calculated using no cells and no protein controls.

In Vivo Pharmacokinetics Studies of EKX-IFN

Animal studies were conducted in accordance with the IACUC protocol using C57BL/6 mice. For all injections 10 µg of protein were injected per animal with three animals per group.

Injections were done retro-orbitally with 100 µL per injection. The initial protein concentration in the serum was determined by blood draw 5 minutes following injection. Blood draws were done by collecting 10-20 µL per animal from the tail of the mice by the tail poke method. Concentrations of HA-IFN and EKX-IFN were determined by ELISA using the LumiKine Xpress hIFN-α- 2.0 kit recognizing human IFN (Invivogen). Blood from PBS- injected mice were used as a control to ensure no cross-reaction with murine IFN. Blood was diluted 500x on ELISA plates. Pharmacokinetic parameters were determined using non-compartmental model.

EKX-IFN Immunogenicity Studies

10 µg EKX-IFN only were injected into mice retro-orbitally once every 10 days for three injections. Blood was harvested 10 days following the final injection. EKX-IFN or IFN alone were coated on RIA/EIA high binding ELISA plates at 50 ng/well in 50 mM sodium bicarbonate pH 9.6 overnight at 4°C. Wells were blocked with 3% BSA in PBS with 0.03% Tween-20 for 2hrs at 37°C. Serum was incubated in wells with the indicated dilutions in blocking buffer for 90 minutes at 37°C. Anti-mouse IgG-HRP or anti-mouse IgM-HRP were diluted in block buffer 1:10,000 and incubated for 90 minutes at 37°C. Plates were developed using 1-step TMB Ultra ELISA solution (ThermoFisher) for 15 minutes. Development was stopped using 2M sulfuric acid and subsequently, absorbance was read at 450nm. Titers were determined by exponential curve fitting and calculated as when OD450 dropped below 0.8.

Results and Discussion

Previously, we purified EKP-IFN expressed in HEK293F mammalian cells. EKP-IFN constructs were ligated to a hemaglutanin (HA) tag on the N-terminus and IFN on the C-terminus. As well, a cleavable transplasminogen activator (TPA) secretion tag was included in the N-terminus, which prompts secretion of HA-EKP-IFN into the expression media allowing for facile purification. This construct was ligated into pcDNA3.1(+) containing the cytomegalovirus (CMV) constitutive promoter (Figure 3-1). To test the effects of glycine and serine composition on the circulation and immunogenicity of zwitterionic peptides, we designed sequences in which half of the proline residues in the original EKP sequence design were substituted with glycine or serine giving rise EKPG and EKPS sequences respectively (Table 3-1). To test the effects of proline composition, we derived the EPKP sequence by inserting proline residues in between the E and K residues from EKP. However, the EPKP repetitive motif was truncated to a 16mer to maintain comparable sequence repetition to the other variants (Table 3-1). The same cloning strategy was followed of EPKP, EKPG, and EKPS (Figure 3-1). Subsequently, these plasmids were transfected into HEK293F mammalian cells and cultured for 4 days, at which point the media was harvested, concentrated, and purified with anti-HA antibody conjugated agarose resin. Purity was analyzed by SDS-PAGE (Figure 3-2a). Apparent molecular weight differences between purified EKX-IFN proteins were observed despite each being nearly the same molecular weight. All constructs ran at a significantly higher molecular weight than the expected molecular weight possibly due to changes in SDS binding.

These proteins were then analyzed by size exclusion chromatography (SEC) to determine their relative hydrodynamic size (Figure 3-2b). EKP-IFN and EKPS-IFN exhibited identical

elution volumes suggesting proline and serine may have similar biophysical effects on the radius of hydration. EPKP-IFN eluted before the other EKX-IFN variants supporting the notion that proline elongates the peptide shape thus increasing the radius of gyration and radius of hydration. On the contrary, EKPG-IFN eluted after EKP-IFN substantiating the hypothesis that glycine collapses the peptide structure and decreases the radius of gyration. All EKX-IFN variants eluted notably earlier than IFN indicating significant increases in apparent molecular weight (Table 3-2).

Differential scanning calorimetry showed EKP-IFN, EPKP-IFN, and EKPG-IFN unfolded at higher temperatures compared to IFN (Figure 3-2c & Table 3-2). EKPS-IFN did not yield a strong minimum in its differential scanning profile possibly due to fluorophore binding to the EKPS domain in the folded state (data not shown). EKP-IFN demonstrated the greatest increase in thermal melting temperature transitioning at 56.7 degrees Celsius, while EKPG-IFN and EPKP-IFN only exhibited modest increases in thermal melting temperature (55.2 and 54.8 degrees Celsius respectively) (Figure 3-2c & Table 3-2). These results are consistent with the stabilizing effects of EK-OPH and EK-β lactamase fusion proteins (Liu & Jiang, 2018; Liu et al., 2015).

The anti-proliferative activity of all EKX-IFN variants on Daudi B cells was significantly reduced compared to IFN alone (Figure 3-2d). There were notable differences between EKX-IFN variants. EKP-IFN exhibited the greatest anti-proliferative activity with an EC50 of 193 +/- 29 nmol/μL. EKPS-IFN and EKPG-IFN displayed modestly reduced anti-proliferative activity compared to EKP-IFN. However, EPKP-IFN showed a more pronounced reduction in anti-proliferative activity exhibiting an EC50 of 2480 +/- 880 nmol/μL (Table 3-2). Steric mechanisms abrogating receptor binding are likely a contributing factor. Still, there are likely other contributing mechanisms as all EKX variants are approximately the same molecular weight. Modeling of EK-ubiquitin suggested EK may induce an allosteric change in structure, which could potentially

explain these results (Shao, 2020). In addition, proline is known to disrupt alpha helix structures (Imai & Mitaku, 2005). As IFN has a significant alpha helix content, the structure disrupting properties of proline could also be contributing to the reduction in activity. This is consistent with the observation that EPKP-IFN had markedly reduced anti-proliferative effects. To abrogate these effects in the future, a flexible glycine serine linker in between the EKX domain and the IFN domain may be able to restore activity.

EKX-IFN proteins were injected into mice intravenously by retro-orbital injection and blood was obtained via the tail poke method at several time points following injection. Anti-IFN sandwich ELISA was used to determine EKX-IFN concentration in the blood following injection to track the EKX-IFN retained in the blood. All EKX-IFN proteins demonstrated increased circulation half-life compare to the short 0.37 +/- 0.02 hour half-life of IFN (Figure 3-3a & Table 3-3). EKP-IFN showed the greatest delay in clearance from the blood exhibiting clearance half-lives 2.55 +/- 0.38 hours compared to EPKP-IFN, EKPS-IFN, and EKPG-IFN, which is reflected in the circulation half-life (Figure 3-3a & Table 3-3). EKX-IFN proteins were injected two additional times in the same mice separated by 10 days in between injections to look for any observable accelerated blood clearance (ABC) effects. EPKP-IFN had no significant ABC effect maintaining a circulation half-life near 2.2 hours for the first and third injection, while EKP-IFN had a slight reduction in circulation half-life for the third injection compared to the first (Figure 3-3b, c, d & Table 3-3). On the other hand, EKPS-IFN and EKPG-IFN displayed a noticeable ABC effect comparing their first injection and third injection circulation time dropping to circulation half-lives of 1.11 +/- 0.07 and 1.25 +/- 0.28 hours respectively (Figure 3-3e, f, & Table 3-3).

As the ABC effect is typically associated with high antibody titers, we collected blood 10 days following the third injection and examined the antibody titers against EKX-IFN. We also

looked at the antibodies directed only against the IFN domain to deduce whether antibodies were binding to the IFN domain or both the EKX and IFN domains. Thus, we coated 96 well plates with EKX-IFN and IFN alone and incubated them with serial dilutions of the collected serum. Then we probed for IgG and IgM bound to both EKX-IFN and IFN alone. EKPG-IFN and EKPS-IFN exhibited higher antibody titers against the EKX-IFN and IFN, which is consistent with the observed ABC effects with these proteins (Figure 3-4a). EPKP-IFN had the lowest antibody titer although the difference was not statistically significant (Figure 3-4a). Titers against the IFN domain showed similar trends as the titers against the whole protein for all EKX-IFN exposed groups (Figure 3-4b). As well, the antibody titers against the IFN domain were consistently lower except for the EPKP-IFN samples (Figure 3-4b). Therefore, other EKX domains may contribute more to the antibody titer than EPKP-IFN. We also examined IgG and IgM levels, which were similar in most cases except for EKP-IFN, which showed higher IgM levels than IgG levels, suggesting EKP may bind to the B cell receptor, induce IgM production, but not trigger class switching (Figure 3-4a & b).

The immunogenicity and pharmacokinetics results need further interpretation as hydrophilicity is presumed to be correlated with reduced immunogenicity and low ABC effects. However, sequences with more hydrophilic glycine and serine inserted into the X position of EKX had higher immunogenicity compared to sequences where X is only proline. Moreover, increasing the proline content with EPKP sequence slightly reduced the antibody titer compared to EKP. These observations suggest that possibly the positioning of the X residue or residues relative to the E and the K may play a significant role. As epitopes are typically short 7-9 amino acids long, the positioning of the juxtaposition of the residues is likely to affect the overall affinity for the B cell receptor, the T cell receptor, and antibodies.

Our results do, however, support the notion that circulation time for the first injection is largely determined by the radius of gyration and hydration. Despite having a larger size observable by SEC, EPKP actually exhibits a shorter circulation time than EKP, suggesting that the greater hydration and zwitterionic content of EKP than EPKP compensates for its reduced size. On the other hand, the smaller size of EKPG, likely due to the biophysical properties of glycine, correlates well to a reduced circulation time.

EKP-IFN *in vitro* anti-proliferative activity and thermal stability superseded that of EPKP-IFN. However, modifications such as including a flexible linker may improve bioactivity, thus warranting further investigation. Most notably, both EPKP and EKP sequences are promising replacements for PEG and present themselves as a viable peptide sequences as a platform for fusion to protein therapeutics.

CONCLUSIONS

Herein, we tested the pharmacokinetics and immunogenicity of four EKX-IFN fusion proteins and characterized their in vitro activities and biophysical properties. EKP-IFN exhibited the best first injection pharmacokinetics and only had a slight decrease in circulation retention for multiple injections. Although EPKP-IFN may have exhibited slightly better repeated injection and slightly lower immunogenicity, the *in vitro* bioactivity of EPKP-IFN is lower than EKP-IFN. The significant reduction in circulation retention and higher antibody titers over multiple injections for EKPS-IFN and EKPG-IFN make these less desirable candidates than EKP and EPKP fused to IFN. The molecular determinants of the immunogenicity of these EKX variants are still being explored. Even so, the ability of EKP-IFN and EPKP-IFN to retain increased circulation time for multiple injections is encouraging. Other strategies can be adopted to address the observed activity losses in these fusion proteins such as including a linker or inserting the EKX domain in another part of the sequence. Activity losses may also be specific to IFN as FDA approved PEGylated IFN exhibits significant activity loss. Overall, appreciably retained pharmacokinetics and low immunogenicity recommend EKP-IFN as a suitable candidate for future trials.

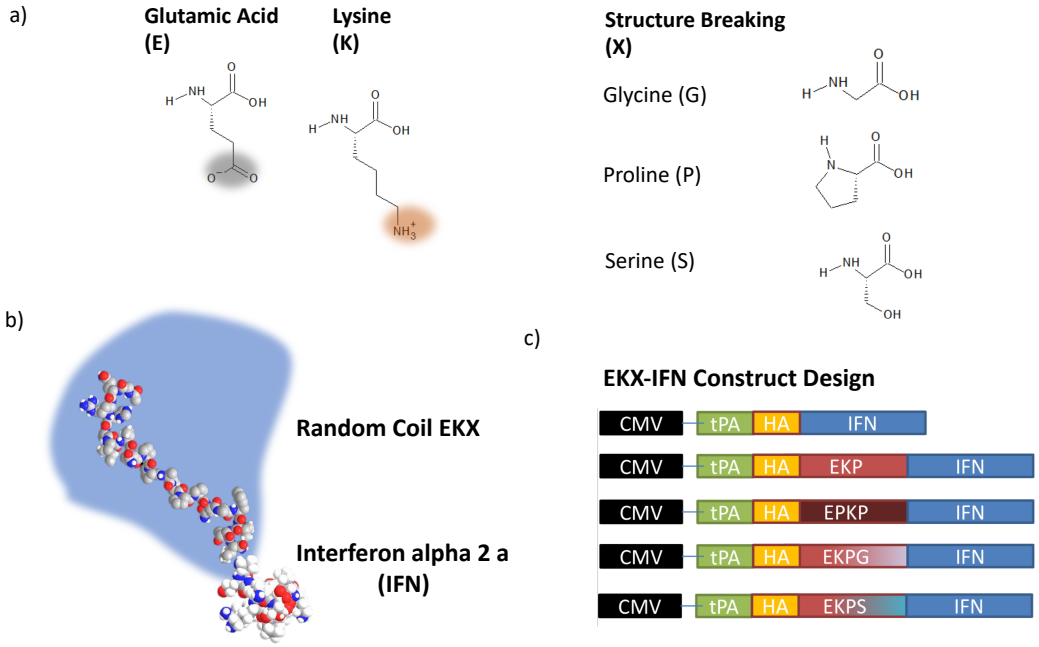

Figure 3-1: (a) Amino acids comprising the different EKX variants as well as their charge or structure breaking properties. (b) A depiction of an expected structure for the EKX fusion protein is also shown, which illustrates its random coil and well hydrated properties. (c) The DNA constructs inserted into plasmids for expression are shown with a CMV promoter, tPA secretion sequence, HA tag for purification, the 30 kDa EKX domain, and IFN domain.

	Sequence	Composition	Theoretical pI	Predicted Secondary Structure
EKP	**EKP**KEPEKPEKPKEPKEP	2**EK** : 1**P**	6.47	100% Coil
EPKP	**EPKP**KPEPKPEPEPKP	1**EK** : 1**P**	6.39	100% Coil
EKPS	**EKPKES**EKPEKSKESKEP	4**EK** : 1**P** : 1**S**	6.47	94% Coil, 6% Helix
EKPG	**EKPKEG**EKPEKGKEGKEP	4**EK** : 1**P** : 1**G**	6.47	100% Coil

Table 3-1: Sequence and properties of EKX domains. Sequences are repeated to comprise a 30 kDa peptide fused to IFN. Theoretical isoelectric point calculated by ExPasy ProtParam. Predicted secondary structure determined by PSIPRED.

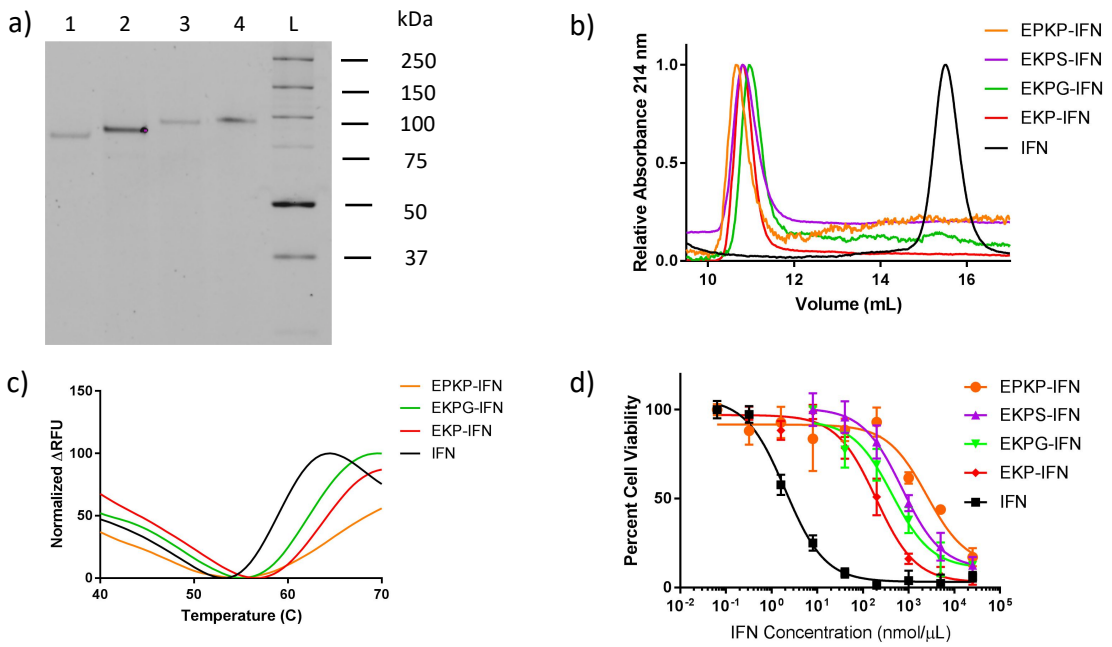

Figure 3-2: Purification and *in vitro* characterization of EKX-IFN. (a) SDS-PAGE gel of EKX-IFN following HA resin purification visualized using No Stain Protein Labeling Reagent (Thermo Fisher). Precision Plus Protein Standards (Bio-rad) was used as the molecular weight standard in Lane L. Lane 1 EKPG-IFN, Lane 2 EKPS-IFN, Lane 3 EPKP-IFN, Lane 4 EKP-IFN. (b) Size exclusion chromatography analysis of EKX-IFN run on Superdex 200 Increase 10/300 GL (GE Healthcare). (c) Normalized change in relative fluorescence units (RFU) of EKX-IFN mixed with SYPRO Orange exposed to a thermal heating gradient obtained using CFX96 RT-PCR machine (Bio-rad). (d) Anti-proliferative activity of EKX-IFN when incubated with Daudi B cells for 96 hours. Proliferation was measured using CellTiter 96 Aqueous solution (Promega).

Protein	EC50 (nmol/µL)	Elution Volume (mL)	Tm (^{o}C)
IFN	2.00 +/- .24	15.53	53.5
EKP-IFN	193 +/- 29	10.81	56.7
EKPG-IFN	430 +/- 130	10.96	55.2
EKPS-IFN	720 +/- 160	10.81	-
EPKP-IFN	2480 +/- 880	10.65	54.8

Table 3-2: *In vitro* properties of IFN and EKX-IFN fusion proteins. Column 1 shows the activity level of IFN and EKX-IFN variants represented by their inhibitory EC50 on the proliferation of Daudi B cells (Figure 3-2d). Column 2 shows the elution volume of IFN and EKX-IFN by size exclusion chromatography (SEC) on a 20 mL Superdex 200 Increase 10/300 GL column (Figure 3-2b). Column 3 shows the thermal melting temperature determined by differential scanning calorimetry (Figure 3-2c).

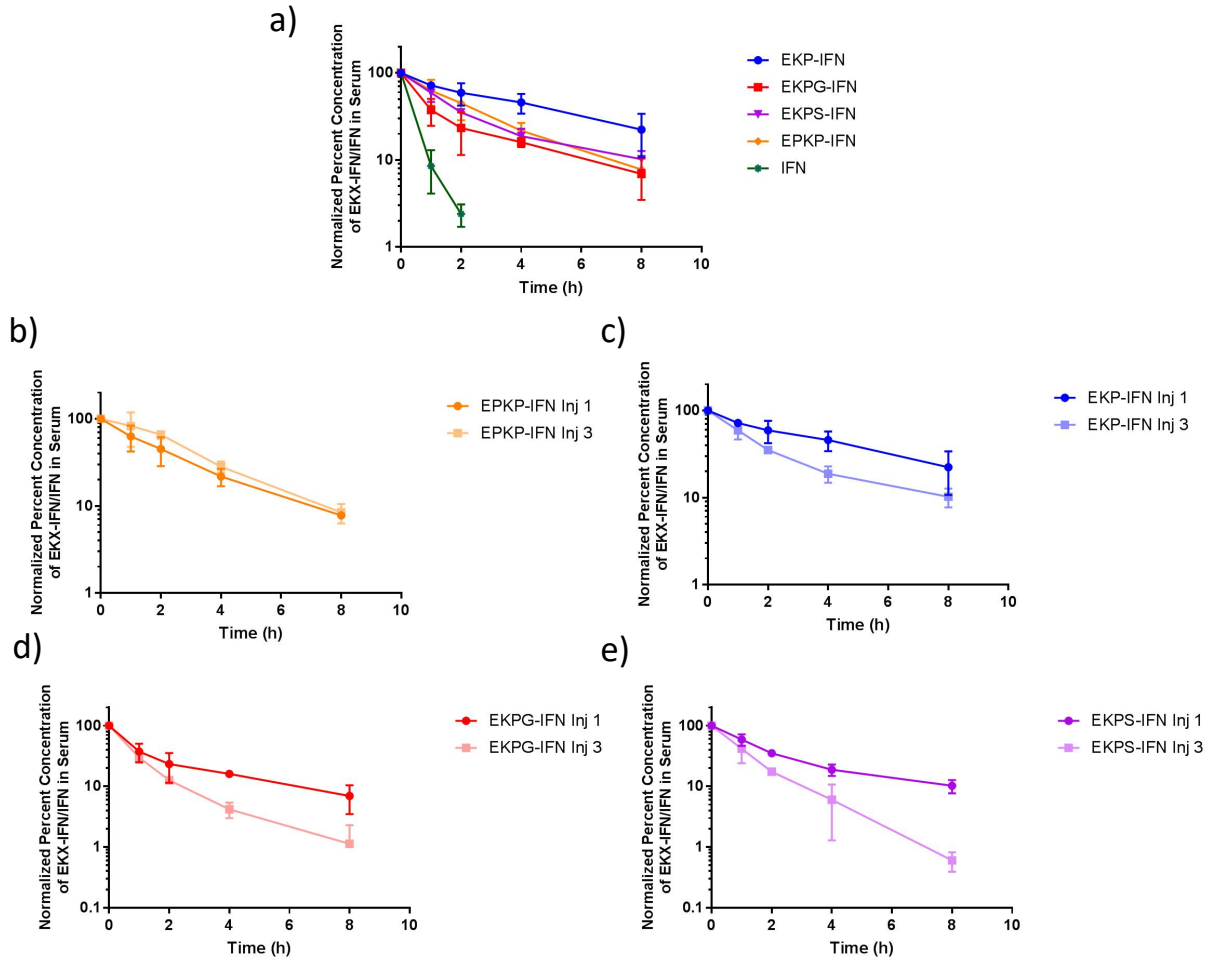

Figure 3-3: Intravenous injection pharmacokinetic profile of EKX-IFN. (a) Normalized concentration of EKX-IFN and IFN in serum following retro-orbital intravenous injection. (b-e) Normalized concentration of EKX-IFN in the serum following retro-orbital intravenous injection for the first and third injection. (b) EPKP-IFN, (c) EKP-IFN, (d) EKPG-IFN, and (e) EKPS-IFN.

Protein	1st Injection Half-Life	3rd Injection Half-Life
IFN	0.37+/- .02	-
EKP-IFN	2.55 +/- .38	2.29 +/- .21
EPKP-IFN	2.20 +/- .18	2.20 +/- .42
EKPG-IFN	2.43 +/- .75	1.25 +/- .28
EKPS-IFN	1.74 +/- .39	1.11+/-.07

Table 3-3: Circulation half-life for EKX-IFN variants for first and third injection. Circulation half-life was determined using non-compartmental pharmacokinetic models.

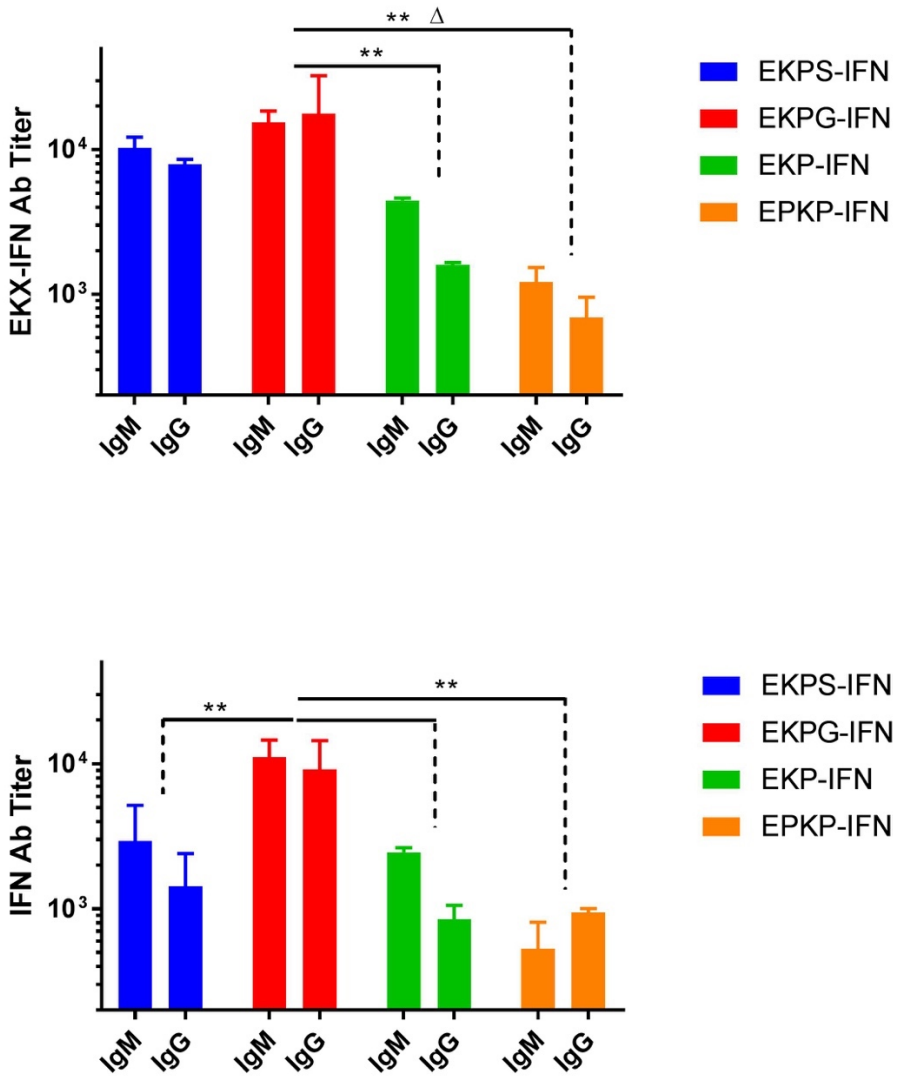

Figure 3-4: Antibody titers following three injections of EKX-IFN. Serum was obtained 10 days following the third injection of EKX-IFN. (a) IgG and IgM antibody titer raised against EKX-IFN. ** indicates p<.005 for IgG. Δ indicates p<.05 for IgM. (b) Antibody titer raised against IFN alone from animals injected with EKX-IFN. ** indicates p<.005 for both IgM and IgG. Comparisons in (a) and (b) done using two-way ANOVA with Bonferonni's multiple comparison test.

CHAPTER 4: DETERMINANTS OF LOW IMMUNOGENICITY OF ZWITTERIONIC PEPTIDES

INTRODUCTION

Highly hydrophilic EK zwitterionic peptides have displayed relatively low immunogenicity. However, zwitterionic peptides mixed with structure disrupting amino acids proline, glycine, and serine were shown to have significant effects on their antibody responses, which were dependent on the composition of structure disrupting amino acids. As the zwitterionic motif is a very specific subset of peptides, the chemical determinants of immunogenicity in peptides exhibiting the zwitterionic motif are incompletely understood.

In fact, the driving forces of immunogenicity have been debated for decades. Hydrophobic and hydrogen bonding interactions are the most prevalent in the antibody antigen likely due to enriched tryptophan, tyrosine, and phenylalanine residues in the Complement Determining Region 3 (CDR3) of the B cell receptor as well as antibodies, which initially interface with the antigen, (Bogan & Thorn, 1998; Ivanov et al., 2005; Martin et al., 2003). The restricted repertoire of amino acids in the CDR3 domain suggest specificity is also predominantly determined by the antigen shape complementary (Calbo et al., 1999; Vargas-Madrazo, Lara-Ochoa, & Almagro, 1995). This is consistent with the observation that increased peptide flexibility correlates with increased antibody binding as a flexible peptide can fit into more diverse CDR3 arrangements (Hogrefe, Kaumaya, & Goldberg, 1989). Furthermore, as the backbone has many hydrogen bond donors and acceptors, it is plausible to reason much of antibody-antigen interactions can be attributed to interactions with the peptide backbone.

Alternatively, ionic interactions driven by electrostatic attraction have also been shown to increase the affinity and specificity of binding (Fukunaga & Tsumoto, 2013). Energetically speaking, electrostatic interactions are long-range and, thus, if present, are likely to initiate an

interaction first (Mihiri Shashikala, Chakravorty, & Alexov, 2019; Z. Zhang, Witham, & Alexov, 2011). Protein-protein interactions, as well as the subset of antigen-antibody interactions, have shown that electrostatic complementarity is a good predictors of binding thus emphasizing its potential role in immunogenicity (McCoy, Chandana Epa, & Colman, 1997). However, electrostatically driven interactions are typically complemented by hydrophobic or hydrogen bonding interactions to stabilize the binding given the lower frequencies of charged amino acids (Fiorucci & Zacharias, 2010; Tsai, Lin, Wolfson, & Nussinov, 1997). Examining these forces within the context of zwitterionic peptides may shed light their determinants of immunogenicity.

Glutamic acid and lysine containing zwitterionic peptides with structure breaking proline, glycine, and serine are subject to potential electrostatic, hydrophobic and hydrogen bonding antibody antigen interactions. Glutamic acid and lysine exhibit reduced hydrophobicity due to their charged domains and will reduce initiating antibody-inducing electrostatic interactions when charge is balanced (Zhu et al., 2016). Serine is also relatively hydrophilic due to its hydroxyl containing side chain but also can participate in hydrogen bonding as a result (Gray & Matthews, 1984). As proline contains a 3 carbon ring side chain, hydrophobicity can contribute to antibody binding, yet its unique imide structure reduces potential hydrogen bonding interactions with the backbone whereas glycine, having no side chain, will exhibit reduced potential for hydrophobic interactions but increased potential for hydrogen bonding interactions (Chakrabarti & Chakrabarti, 1998; Kay, Williamson, & Sudol, 2000; Nozaki & Tanford, 1971).

The breadth of potential forces driving zwitterionic peptide antibody antigen obscure the underlying mechanism of their immunogenic behavior. Detailed characterization of the interaction types and contributions from each amino acid would require hybridoma cell lines to be established and crystal structures of antibody antigen complexes for zwitterionic peptides and the

corresponding antibodies to solved, which is extremely laborious (Davies & Cohen, 1996). Alternatively, epitope mapping and alanine scanning experiments offer quicker alternatives to infer a potential driving forces (Moreira, Fernandes, & Ramos, 2007). Herein, we conduct epitope mapping and alanine scanning experiments to examine antibodies from mice injected to with zwitterionic peptide fusion proteins that recognize their respective zwitterionic peptides, specifically, EKP-IFN, EPKP-IFN, EKPG-IFN, and EKPS-IFN. Based on these results, we designed further *in vivo* immunogenicity tests to understand the effects of E and K position and distance with respect to the structure breaking amino acids P, S, and G.

MATERIALS AND METHODS

Epitope Mapping and Alanine Scanning of Genetically Engineered EKX

Peptides were synthesized using on TOTD membranes containing a PEG linker via the SPOT synthesis method courtesy of Kinexus Bioinformatics Inc. Membranes were blocked with 3% BSA in PBS/0.03% Tween-20 for two hours at room temperature. Then, membranes were incubated with 1:200 dilution of serum in block buffer for 90 minutes at room temperature. Serum was obtained from mice injected 3x with EKX-IFN. Serum from animals in each group was mixed to get a representative sample of all animals from each group on one membrane. Anti-mouse IgG-HRP was diluted 1:2000 in block buffer and incubated for 90 minutes at room temperature. Membranes were developed using 1-Step TMB Blotting solution (ThermoFisher). Development was stopped using water and imaged immediately. Signal intensity was determined using ImageJ analysis.

EKX-KLH Immunogenicity Screen

Peptides were synthesized using standard fmoc tert-butyl chemistry and linked to cysteine residues using β alanine linkers (5mers). Then, they were conjugated using NHS-EDC chemistry to either KLH or BSA or were not conjugated at all (free form). Peptide synthesis and conjugation were done courtesy of Kinexus Bioinformatics Inc.

30 μg of EKX-KLH or KLH or PBS control were injected subcutaneously into mice. A second injection was done 2 weeks following the first injection with the same concentration. One week following the second injection serum was collected from all mice via the chin bleed method to determine antibody titers.

To determine the antibody titer specifically against the EKX domain, EKX-BSA was coated on RAI/EAI high binding ELISA plates 300 ng/well in 50 mM sodium bicarbonate pH 9.6 overnight at 4°C. Wells were blocked with 3% BSA in PBS with 0.03% Tween-20 for 2hrs at 37°C. Serum was incubated in wells with the indicated dilutions in blocking buffer for 90 minutes at 37°C. Anti-mouse IgG-HRP or anti-mouse IgM-HRP were diluted in block buffer 1:10,000 and incubated for 90 minutes at 37°C. Plates were developed using 1-step TMB Ultra ELISA solution (ThermoFisher) for 15 minutes. Development was stopped using 2M sulfuric acid and subsequently, absorbance was read at 450nm. Titers were determined by exponential curve fitting and calculated as when OD450 dropped below 0.8.

Cross reactivity test of EKX peptides

Cross reactivity experiments were conducted similar to antibody titer experiments by the ELISA method. However, only six EK variants were considered: the i+1 and i+2 variants with no X, P, and G. For each serum sample, the cross reactivity with the three most similar peptides were tested. To obtain the data shown in the plot, serum samples from injected animals were mixed to get a representative average and the average of three technical replicates is shown. Briefly, BSA-EKX conjugated peptides were coated on ELISA plates, and serial dilutions of antibody containing serum were incubated with ELISA coated plates. The antibody binding titer was determined as previously described. To determine antibody cross reactivity score, the antibody binding titer was normalized to the average antibody binding titer for all samples tested, thus allowing for comparison of antibody binding to EKX peptides, which were generated against other EKX variants.

Results and Discussion

Previously we examined the immunogenicity of genetically engineered EKX peptides. To examine the driving factors of immunogenicity in EKX peptides, we conducted alanine scanning experiments using spot peptide synthesis to examine trends in antibody binding to EKX sequences. As these sequences were made by repeating 18mers (16mer for EPKP), we reasoned six 9mer (four 12mers for EPKP) peptides would recapitulate all possible epitopes for each sequence (Figure 4-1). For alanine scanning, we substituted alanine at each position in the 9mer or 12mer sequences. 9mer (or 12mer for EPKP) peptides were synthesized and immobilized on cellulose membranes by peptide spot synthesis (Figure 4-1). Membranes were incubated from serum obtained following three injections of EKX-IFN 10 days apart and collected 10 days following the third injection. Then, membranes were probed for binding of mouse IgG to these peptides using anti-mouse IgG antibody conjugated to HRP. We selected IgG as opposed to IgM as IgG tends to have greater specificity of binding compared to IgM and thus, will show clearer trends. Then, these membranes were developed using TMB western blotting substrate and imaged. Binding intensity was determined by ImageJ analysis quantifying the extent of deposition of the substrate on the membrane. Changes in binding intensity due to insertion of alanine residues were normalized to the intensity of the sequence without the alanine substitution (one of the six 9mers or four 12mers for EPKP).

To determine binding trends, we first looked at the relative change in binding induced by alanine substitution as per each amino acid (i.e., E, K, P, etc.). In most cases except for EKP, changing glutamic acid to alanine resulted in increased binding of antibodies to the peptide (Figure 4-2a-e). Except for EPKP, changing lysine to alanine resulted in decreased antibody binding

(Figure 4-2a-e). As these are averaged values, they may hide trends due to sequence-specific difference. Therefore, we examined the alanine substitutions individually and grouped each substitution according to the parent sequence and the amino acid change (Figures 4-2f-h). When examining the alanine substitutions individually, glutamic acid to alanine changes still showed increased antibody binding, while lysine to alanine changes showed decreased antibody binding. The only exception is EKP, in which changes in glutamic acid and lysine to alanine both decrease antibody binding (Figure 4-2f). Mild sequence-specific differences were observed with EKPS and EPKP (Figure 4-2c & g). These data suggest lysine residues are more prone to antibody binding, while glutamic acid residues seem to prevent antibody binding except for in the case of EKP in which lysine and glutamic acid seem to contribute to the immunogenicity equally. Alternatively, the anti-EKP antibody specificity may be greater than the other EKX variants potentially due to unique structural properties of EKP. Furthermore, on average proline, glycine, and serine residues when changed to alanine did not significantly change the antibody binding suggesting that these residues alone are not major contributors to immunogenicity. However, the profound changes in antibody titers from changes in the identity of X in the EKX sequence suggest the impacts of proline, glycine, and serine on the surrounding glutamic acid and lysine residues may be contributing to immunogenicity.

Suspecting that the relative positioning of glutamic acid and lysine has a significant impact on immunogenicity, we wanted to more systematically explore these effects. Previous structural analysis has shown that glutamic acid and lysine residues separated by two (i+3) or three (i+4) residues can form salt bridges (Figure 4-3) (Marqusee & Baldwin, 1987). In addition, as amino acid side chains are typically in the *trans* position, EK juxtaposed in the primary amino acid sequence (i+1) may actually cause greater charge separation and areas with high electrostatic

potential compared to those separated by several residues (Figure 4-3). Because proline, serine, and glycine disrupt structure by different mechanisms, we reasoned that these amino acids would have impacts on the rotation of the glutamic acid and lysine side chains. To address this more systematically, we composed a positional (i+1 to i+4) and rotational (P,S,G) EKX matrix to examine the sequence dependence of EKX (Figure 4-3 table).

12mers or 16mers of these sequences were synthesized and conjugated to keyhole limpet hemocyanin (KLH) protein, which is a highly immunogenic protein typically used as a carrier to increase antibody titers for polyclonal antibody production. This effectively pushes the immunogenic potential to the extreme to elucidate subtle differences in peptide immunogenicity, which is necessary given the sequence similarity of the EKX peptide matrix. KLH-EKX conjugates were injected twice, two weeks apart, and serum was collected one week after the second booster injection to collect the peak of antibody production. Antibody titers against the EKX domains were tested by coating BSA-EKX conjugates on ELISA plates. EKS (i+1) and EKG (i+1) showed higher IgG and IgM titers, while EKP (i+1) and EK (i+1) exhibited reduced antibody titers which is consistent with the EKP, EKPS, and EKPG antibody titers from EKX-IFN fusion proteins (Figure 4-3a & b). As well, reduced antibody titers with EK (i+1) are consistent with EK previously conjugated to asparaginase, another known immunogenic therapeutic protein. i+3 and i+4 EKX variants typically exhibited higher antibody titers except for i+3 and i+4 variants of EKG (Figure 4-3a & b). However, i+2 variants of EK, EKP, EKS, and EKG all showed lower immunogenicity (Figure 4-3a & b). As i+3 and i+4 variants are expected to form internal salt bridges, this suggests that salt-bridging may have a positive correlation with higher immunogenicity. The stark differences in antibody titers at the i+1 position could be explained by hydrogen bonding interactions between the antibody and the peptide backbone. For EK (i+1), the

backbone could be protected by the zwitterionic side chains, however, when glycine, proline, and serine are inserted, the backbone becomes exposed allowing for hydrogen bonding to the amide. The unique imide bond of proline eliminates the hydrogen bonding acceptor character at these exposed positions, while the amide bond in the glycine and serine has both hydrogen bond donor and acceptor potentials. This is consistent with the proposed anti-fouling rules put forth by George Whiteside and coworkers, who suggested that hydrogen bond donors are more fouling than hydrogen bond acceptors (Chapman et al., 2000; Ostuni, Chapman, Holmlin, Takayama, & Whitesides, 2001). The observed low immunogenicity of EKG i+3 and i+4 variants may be due to the backbone flexibility from glycine allowing E and K to rotate allowing better protection of the backbone.

To try to better understand the molecular determinants of low immunogenicity, we examined the cross reactivity of the antibodies from the i+1 and i+2 variants of EK, EKP, and EKG as these contained the lowest immunogenicity sequences. To limit the number cross-reactive combinations to test, we only examined the cross reactivity between i+1 and i+2 of the same rotational variant or between the same positional variants (Figure 4-3a). EK and EPKP antibodies showed lower cross reactivity compared to the others, while EGKG showed the highest possibly due to differences in flexibility of EGKG compared to the others (Figure 4-3b). EKP peptide showed the lowest cross reactivity to the other antibodies possibly due to its conformational inflexibility, while EPKP showed slight increases in cross reactivity possibly due to its hydrophobicity (Figure 4-3b). This reveals an interesting dichotomy of EGKG despite being less antigenic, generates antibodies that have greater cross reactivity. On the other hand, EKG, despite being more antigenic, generates antibodies that are less cross reactive (Figure 4-2a &b, Figure 4-3b). The lower cross reactivity suggests a potentially unique structure of EKP compared to the

other EKX sequences. Importantly, this EKX screen points to sequence patterns for future exploration of low immunogenicity peptides. Specifically, i+2 EKX peptides tended to exhibit lower immunogenicity compared to the others suggesting other amino acids may be inserted into these positions to drive immunogenicity down even further.

CONCLUSIONS

In this chapter, we explored the determinants of EKX immunogenicity by epitope mapping and alanine scanning experiments to probe the antibodies produced by EKX-IFN injected animals. These studies revealed that glutamic acid to alanine substitutions tended to increase antibody binding, while lysine to alanine substitutions tended to decrease antibody binding. Moreover, proline, glycine, and serine to alanine substitutions did not show any strong trends despite their significant impacts on immunogenicity observed in EKX-IFN fusion proteins. Therefore, based on these observations, we speculate that the juxtaposition of E and K with respect to X and the impact of X on the positioning of the E and K side chains may be significant determinants of immunogenicity. To test this, we designed EKX matrix with positional variants (i+1 to i+4) and rotational variants (P,G, & S) to examine for the trends that may be leading to high or low immunogenicity. i+1 variants of EK and EKP exhibited low immunogenicity, while that of EKG and EKS exhibited high immunogenicity, which is consistent with the antibody titers observed with EKX-IFN variants. All of the i+2 variants, including EPKP, exhibited relatively low immunogenicity, while the i+3 and i+4 variants tended to have higher immunogenicity except EKG i+3 and i+4. These trends suggest that hydrogen bonding interactions with the backbone may be contributing to immunogenicity in addition to hydrophobicity, charge distance, and flexibility. Evidence of these mechanisms are also apparent in the cross reactivity of EKX antibodies and peptides.

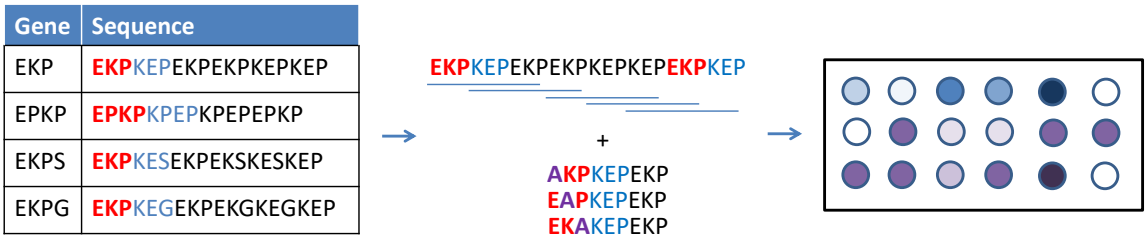

Figure 4-1: Schematic of epitope mapping and alanine scanning experiments using peptide spot synthesis on cellulose membranes. The table to the left shows all sequences that were injected separately into mice as genetic fusions to IFN. The diagram in the middle demonstrates the strategy to map and scan the EKP sequence as an example. Briefly, for epitope mapping six 9mer sequences spanning the entire repeating 18mer EKP sequence were identified. Then, each residue in the 9mer was individually changed to alanine generating 9 alanine variant sequences for each 9mer and 54 alanine variants for the entire EKP. The schematic on the right is a representative diagram of the membrane following probing with the antibody. Darker color indicates higher antibody binding.

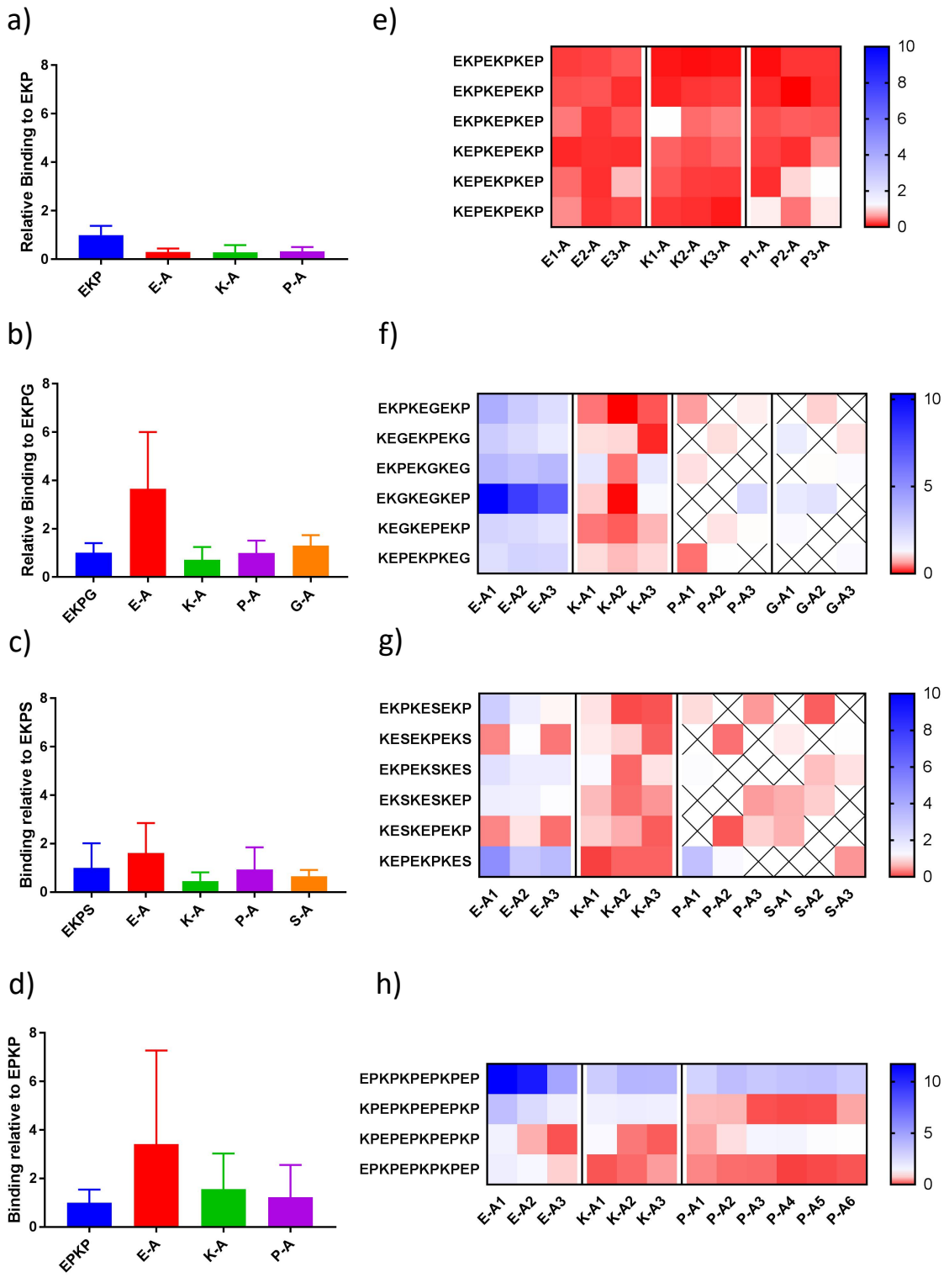
a)
Relative Binding to EKP
EKP
E-A
K-A
P-A
b)
Relative Binding to EKPG
EKPG
E-A
K-A
P-A
G-A
c)
Binding relative to EKPS
EKPS
E-A
K-A
P-A
S-A
d)
Binding relative to EPKP
EPKP
E-A
K-A
P-A
e)
EKPEKPKEP
EKPKEPEKP
EKPKEPKEP
KEPKEPEKP
KEPEKPKEP
KEPEKPEKP
E1-A
E2-A
E3-A
K1-A
K2-A
K3-A
P1-A
P2-A
P3-A
f)
EKPKEGEKP
KEGEKPEKG
EKPEKGKEG
EKGKEGKEP
KEGKEPEKP
KEPEKPKEG
E-A1
E-A2
E-A3
K-A1
K-A2
K-A3
P-A1
P-A2
P-A3
G-A1
G-A2
G-A3
g)
EKPKESEKP
KESEKPEKS
EKPEKSKES
EKSKESKEP
KESKEPEKP
KEPEKPKES
E-A1
E-A2
E-A3
K-A1
K-A2
K-A3
P-A1
P-A2
P-A3
S-A1
S-A2
S-A3
h)
EPKPKPEPKPEP
KPEPKPEPEPKP
KPEPEPKPEPKP
EPKPEPKPKPEP
E-A1
E-A2
E-A3
K-A1
K-A2
K-A3
P-A1
P-A2
P-A3
P-A4
P-A5
P-A6

Figure 4-2: Epitope mapping and alanine scanning results of EKX genes. All binding intensities shown determined by imageJ and normalized to the parent 9mer of EKX (peptide without alanine substitution) (a-d) Bar graphs show average binding intensities for glutamic acid to alanine (E-A), lysine to alanine (K-A), proline to alanine (P-A), glycine to alanine (G-A), or serine to alanine (S-A). Average binding intensity of antibody to parent EKX sequence shown for comparison. (e-h) Binding intensities of alanine scanning variants for all EKX. Blue indicates increased antibody binding following alanine substitution. Red indicates decreased binding following alanine substitution.

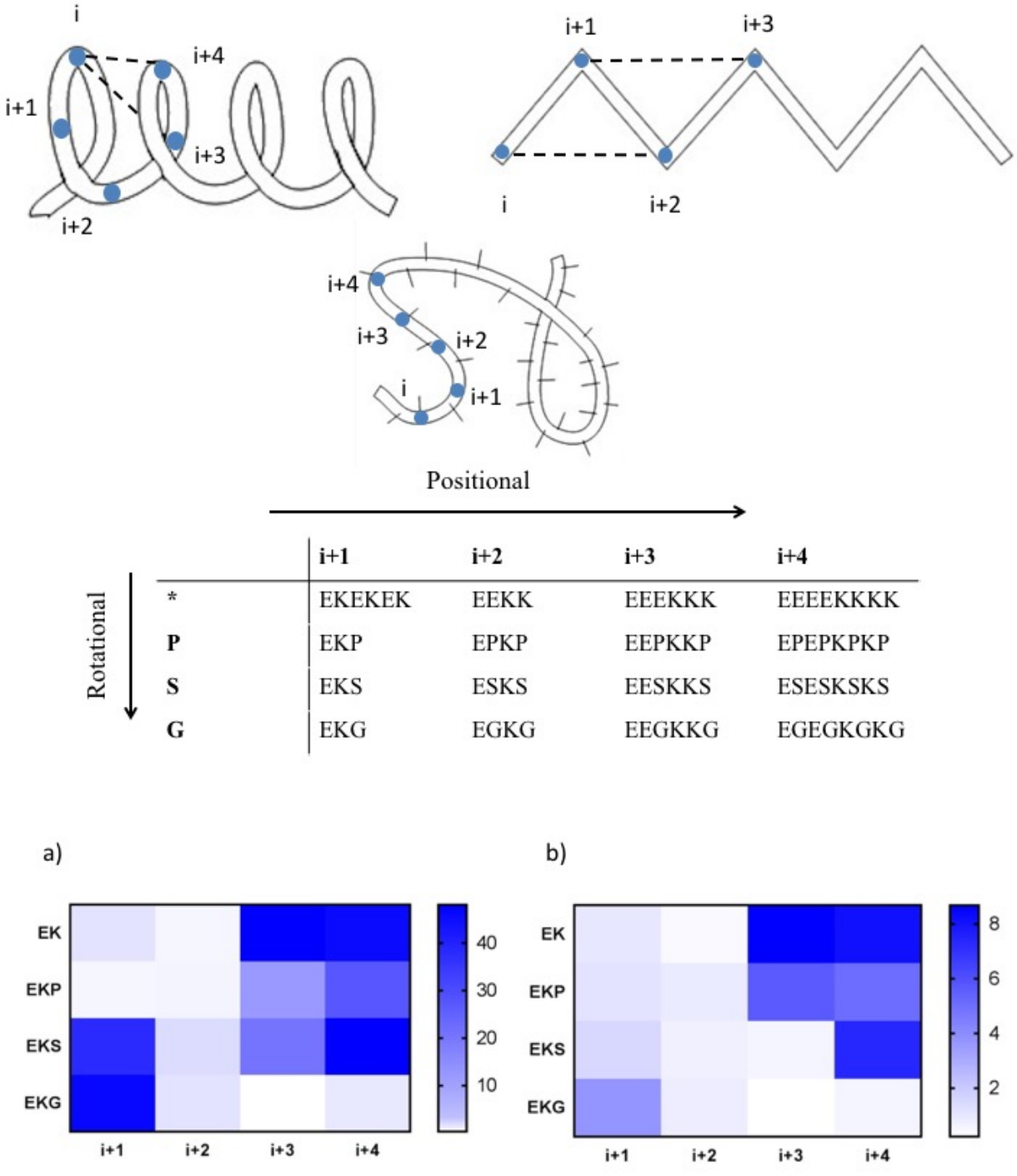

	i+1	i+2	i+3	i+4
*	EKEKEK	EEKK	EEEKKK	EEEEKKKK
P	EKP	EPKP	EEPKKP	EPEPKPKP
S	EKS	ESKS	EESKKS	ESESKSKS
G	EKG	EGKG	EEGKKG	EGEGKGKG

Figure 4-3: Top of diagram depicts possible interactions between E and K side chains depending on structure (ie alpha helix, beta sheet, or random coil). Middle of diagram depicts the systematic

approach to probe different positional (i+1 to i+4) and rotational variants (P, S, and G). Sequences in the table were conjugated as either 12mer or 16mer repeats to KLH and injected twice subcutaneously into mice. Bottom of the figure shows antibody titers for KLH-EKX injected mice that target the EKX domain. Antibody titers were normalized to KLH-EK antibody titers and the fold change in antibody titers are depicted (darker blue indicates greater antibody titer). (a) Shows IgG (b) Shows IgM .

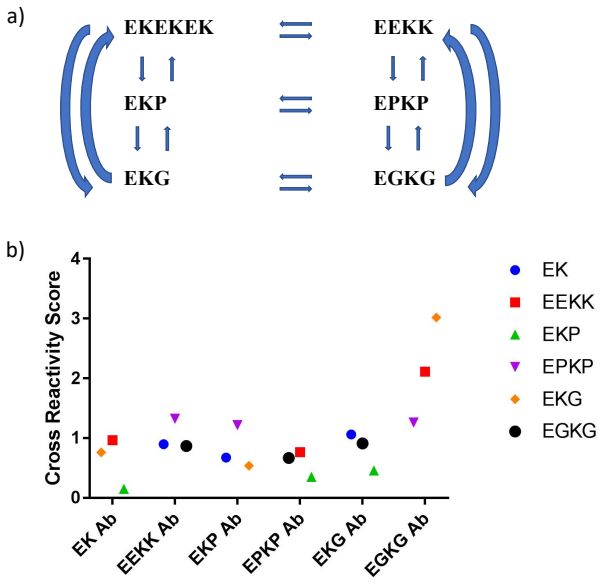

Figure 4-4: Cross-Reactivity of EKX i+1 and i+2 with proline and glycine variants. Cross reactivity of within rotational variant (*, P, G) was compared between positional variants i+1 and i+2. Cross reactivity within positional variant (i+1 or i+2) was compared between rotational variants * (meaning no P or G), P, and G. The x-axis shows the EKX variant that was injected into the mice. The colored/shaped labels indicate the sequence with which the indicated antibodies cross react. The cross-reactivity score indicates the antibody binding titer by ELISA normalized to the average of all antibody titers.

CHAPTER 5: SCALED PRODUCTION OF HIGH DENSITY POLYCARBOXYBETAINE ORGANOPHOSHATE HYDROLASE CONJUGATES

INTRODUCTION

Organophosphate (OP) compounds are a pressing concern in today's world as they have been used with malevolent intent as chemical warfare nerve agents. In addition, OPs are used as pesticides and, thus, pose a risk to farmers and crop harvesters that are exposed to these toxic compounds (Eddleston, Buckley, Eyer, & Dawson, 2008). Therefore, there exists an increasing need for long term protection against OP compounds. These chemicals have been shown to irreversibly bind acetylcholinesterase, which results in build-up of acetylcholine resulting in depression in respiration, tremors, salivation, and eventually death if sever enough (Trovaslet-Leroy et al., 2011). Strategies to combat the effects of OPs have primarily focused on butylcholinesterase, which only binds to OP compounds in one to one stoichiometric ratio (Trovaslet-Leroy et al., 2011; P. Zhang et al., 2016). However, recent attention has been drawn to organophosphate hydrolase (OPH) because it has catalytic activity against OPs and, thus, can actively breakdown OPs thereby more efficiently combating their toxicity(Wales & Reeves, 2012).

Despite the promising properties of this protein, OPH is derived from prokaryotes and is, thus, highly immunogenic. Furthermore, OPH is a membrane protein and has evolved to have many hydrophobic surface residues, which increases macrophage uptake and reduces its in vivo half-life (Novikov, Grimsley, Kern, Wild, & Wales, 2010; Wales & Reeves, 2012). Therefore, to take advantage of OPH, the surface residues must be protected by using well hydrated polymers to protect the hydrophobic surface residues and reduce macrophage uptake. In addition, protecting the surface residues will prevent antibody binding that has been shown to facilitate accelerated blood clearance upon multiple injections of the highly immunogenic protein.

Herein, OPH production was scaled up by developing a bioreactor expression protocol to achieve high density *E. coli* cultures and adapt the existing purification methods to accommodate larger protein quantities. In addition, purification protocols were developed after conjugation of the PCB polymer to OPH to isolate high density PCB-OPH. High density PCB-OPH conjugates are expected to better increase the in vivo circulation half-life of OPH and show improved protection against nerve agent challenge. These results have promising applications in chemical warfare to protect soldiers from unexpected nerve agent attacks for multiple weeks.

MATERIALS AND METHODS

Plasmids Construction

DNA sequences encoding organophosphate hydrolase with mutations for enhanced activity toward G-type nerve agents (YT) were cloned into pET20b+ plasmids courtesy of Andrew Bigley from Texas A&M University. These plasmids were transformed into BL21 (DE3) *E. coli*.

OPH Expression Conditions

40 mL starter cultures in LB/amp were incubated overnight at 37 C. Subsequently, they were transferred to 1L of TY media in 2.5 L bioreactor vessel. The culture was incubated at 30C with 500 rpm agitation and 2.5 L/min aeration. When OD600 reached .75, 1 mM IPTG was added to induce expression with 1 mM CoCl2. At this point, 2x TY feed media was started for the culture at 10% speed. Feed media was added until it 1L was added (~10 hr). Then, the culture was continued for another 14 hr and harvested by centrifugation.

OPH Purification

Pellets were resuspended in ~500 mL of 50 mM HEPES .1 mM CoCl2 pH 8.5. Then the suspended bacteria were lysed by sonication and clarified by centrifugation. The supernatant was then diluted to 1 L with buffer. Nucleic acids were removed by precipitation with 2 g/L of protamine sulfate. Subsequently, YT was precipitated by ammonium sulfate precipitation at 60% saturation. The protein was isolated by centrifugation and redissolved in HEPES/CoCl2 buffer. The solution was then dialyzed overnight against HEPES/CoCl2 buffer to remove trace amounts of ammonium sulfate allowing for unstable contaminates to precipitate. The resulting protein

solution was applied to 90 mL anion exchange column packed with Capto Q resin (GE). OPH-YT does not bind to resin, while contaminants and endotoxins bind.

OPH-YT was washed several times with Amicon 30 kDa centrifuge protein concentrators. Then concentration was adjusted to ~5 mg/mL at which point it was precipitated using cold 80% ethanol to remove contaminating lipids. The protein was resuspended in buffer again and washed several times to remove trace quantities of EtOH. Finally, trace quantities of endotoxin were removed using .5% triton x-114 phase separation. The aqueous phase was isolated and the phase separation was repeated until only the aqueous phase was visible. Then the resulting protein was washed several times to eliminate trace quantities of Triton X-114.

PCB-OPH conjugation conditions

20 kDa polycarboxybetaine with a free thiol (PCB-SH) was synthesized as described by Li *et al* and provided by Dr. Zhefan Yuan. For the conjugation reaction, AMAS (ThermoFisher) was dissolved in DMSO at 40 mg/mL and added to 2 mg/mL OPH in 50 mM HEPES with .1 mM CoCl2 for ~2 fold excess AMAS per available lysine, which equates to 3.1 μL of 40mg/mL in DMSO to 1mL OPH at 2mg/mL. The reaction was done at room temperature for 1 hour. The solution was washed three times with 30 kDa cutoff ultrafiltration protein concentrator with 50 mM HEPES buffer pH 7 with .1mM CoCl2. 40 mg/mL of PCB-SH was dissolved in buffer. 40 mg of PCB-SH was reacted with 1mg of OPH. The reaction was done at room temperature for 2h hours. Free polymer was eliminated using 100 kDa ultra centrifuge filters and washed several times with 50 mM HEPES .1mM CoCl2 pH 7.2.

Purification of High Density and Low Density PCB-OPH

After conjugation, PCB-OPH conjugate samples were applied to a HiScale column packed with 50 mL of CaptoButyl Resin (GE HealthCare). The column was equilibrated with 50 mM HEPES pH 7.2, .1mM CoCl2, 2M NaCl. PCB-OPH conjugate samples were diluted 2x with 4M NaCl and HEPES buffer to increase the NaCl concentration to 2M. These samples were applied to the captoButyl resin at a protein concentration of 5 mg/mL and a flow rate of 2 mL/minute. 100 mg of PCB-OPH was applied per run. PCB-OPH that did not bind to the captoButyl resin was considered high density PCB-OPH. Residual unconjugated PCB-SH eluted slightly later than PCB-OPH likely due to partial hydrophobicity of SH moiety. A decreasing NaCl gradient from 2M to 0M over 2 column volumes was applied to the column.

Michaelis Menten Enzyme Kinetic Parameters

50 ng/mL of OPH, low density and high density PCB-OPH was dissolved in 10 mM MOPS pH 7.0, 100 μM CoCl2, with .1mM to 2 mM Paraoxon. The conversion of paraoxon to p-nitrophenol was determined by the absorbance at 405nm on the BioTek Cytation 3 plate reader. The Vmax values were determined with 1 mM Paraoxon.

Results and Discussion

Previous work from Zhang et al demonstrated the promising applications of PCB to protect OPH for improved scavenging of organophosphates. However, this work focused on a nanogel formulation of PCB-OPH, which produced a much larger nanoparticle that is not as easily degraded by the body resulting in potential accumulation and may increase size dependent macrophage uptake (Soni, Desale, & Bronich, 2016). Therefore, producing a smaller, yet well protected PCB-OPH conjugate is more desirable and may have improved protection. Achieving a conjugate PCB-OPH formulation required scaling up OPH production capabilities due to incomplete conjugation of PCB to lysine residues on the protein. Because PCB is ultrahydrophilic and OPH is more hydrophobic, their interaction is not particularly favorable making conjugation less efficient, and, thus, requiring scaled-up production of OPH compared to the previous shaker flask OPH expression and purification protocol (Bigley, Mabanglo, Harvey, & Raushel, 2015). To do so, a fed batch bioreactor expression protocol was established for OPH capable of producing 2L of high density *E. coli* cultures using TY media and 2x TY media as the feed media based (Tripathi, Shrivastva, Biswal, & Rao, 2008). This allowed for rapid expression of greater than 350 mg of OPH per 2L expression batch in the bioreactor.

Previously, we were only able to achieve 50 mg per batch of *E. coli* culture by using shaker flasks. To accommodate the increased expression capabilities, we redesigned the purification protocol to accommodate the scaled-up expression. Previously the purification protocol relied on size exclusion chromatography (SEC). We encountered significant difficulties with this step as contaminants were binding to the SEC column and significantly inhibiting the purification process. Moreover, this step was particularly slow requiring at maximum capacity 2-3 hours per run and sub-optimally 5-7 hours that only yielded around 15 mg of OPH per run. As a result, we were only

able to comfortably produce 50 mg of OPH per week, thus, significantly hindering the amount of PCB-OPH conjugate that could be produced.

To circumvent these issues, the protein was dialyzed to eliminate small contaminants, which also allowed for unstable contaminants to precipitate out allowing for the complete elimination of the SEC step and going directly to the anion exchange step. With the previous purification protocol, we noticed severe fouling of the small anion exchange column after multiple batches of OPH causing protein loss. This issue was only exacerbated at large scale resulting in constant replacement of the anion exchange resin. Therefore, the process was altered to include a prewash with small a small quantity (about 5 mL per batch) of anion exchange resin on a gravity column before applying to the anion exchange column on the FPLC, thus saving time of unpacking and repacking the column.

Previous conjugation reactions of PCB with OPH purified using the original protocol, exhibited significant precipitation with the addition of the AMAS crosslinker. We initially suspected that this was due to unfolded protein. However, at scale, this problem was significantly worse and the specific activity of the protein was similar indicating that another contaminant could be causing the problem. As OPH is a hydrophobic protein, we suspected lipid contamination. Therefore, an ethanol precipitation step was implemented to eliminate possible lipid contaminants. This significantly abrogated the precipitation issues in the crosslinker conjugation step.

With these adaptations to the purification protocol, we were able to achieve approximately 350 mg of OPH per 2L batch in the bioreactor. Moreover, it is likely this process could be easily scaled to accommodate a 5L or 10L bioreactor system and achieve greater than gram scale yields without significant changes to the protocol.

Purified OPH was then conjugated a 20 kDa PCB to OPH targeting lysine residues on OPH using AMAS, which is an NHS ester maleimide heterobifunctional cross-linker. There are five available lysine residues on the surface of organophosphate hydrolase (Novikov et al., 2010). NHS esters react with the primary amines from the lysine residues at pH 7-9. The maleimide group reacts with thiol groups on PCB-SH at pH 6.5-7.5 to forms thiol ester linkage to conjugate PCB to OPH. The reaction was performed in HEPES buffer pH 7.2 allowing for the reaction of the NHS ester. Then, the pH was reduced to 7.0 for the thiol ester reaction of PCB-SH with a minimal pH shift as large shifts in pH can destabilized the protein. As uncovered hydrophobic moieties are not desirable, we purified the conjugated protein using hydrophobic interaction chromatography (HIC) to isolate partially conjugated and fully conjugated PCB-OPH. The fully conjugated or high-density PCB-OPH was suspected to not bind to the HIC column, but the partially conjugated PCB-OPH or low-density PCB-OPH was expected to bind and elute using lower salt concentrations. Moreover, the unconjugated OPH would elute with much lower salt concentrations or no salt thus allowing for removal of unconjugated OPH and isolation of low density and high density conjugated PCB-OPH.

To confirm the isolation of these subpopulations, high density conjugated PCB-OPH, low density PCB-OPH, and bare OPH were analyzed by gel permeation chromatography (GPC), which revealed that a large increase in hydrodynamic radius with conjugation of PCB (Figure 4-2). Furthermore, we see a difference in size with the low density and high density OPH-PCB as more PCB polymer chains increase the particle size, thus, validating that we isolated low density and high density PCB-OPH conjugates.

To examine the effect of the PCB polymer on the activity of OPH, the Michaelis-Menten parameters for OPH to catalyze the breakdown of paraoxon were tested (Figure 4-3). A decrease

in the Michaelis constant with an increase of PCB conjugation was observed suggesting there is less binding of paraoxon to the enzyme active site with a 40% decrease Km with high density PCB conjugation. The Vmax and catalytic turnover numbers (kcat) also showed a decrease. However, the kcat/Km ratio was relatively similar to OPH and PCB-OPH conjugates suggesting the decrease in turnover number and maximum velocity is largely due to reduced paraoxon binding with pCB-OPH conjugates.

CONCLUSIONS

In this work, PCB conjugated to OPH was shown to improve the organophosphate scavenging capabilities of OPH *in vivo*. This was accomplished by increasing the OPH production capacity requiring improved expression and purification techniques. In doing so, OPH expression was increased to 350 mg per batch where the previous methods only 50 mg per batch. Furthermore, improved purification techniques were developed to isolate highly conjugated PCB-OPH proteins. As a result, high density PCB-OPH was shown to increase the circulation time compared to OPH and maintain similar pharmacokinetics after multiple injections. Finally, it was shown that PCB-OPH can prophylactically protect rats up to eight days from paraoxon poisoning. These results reveal the potential application of PCB-OPH to protect soldiers on the battlefield against unexpected nerve agent attacks.

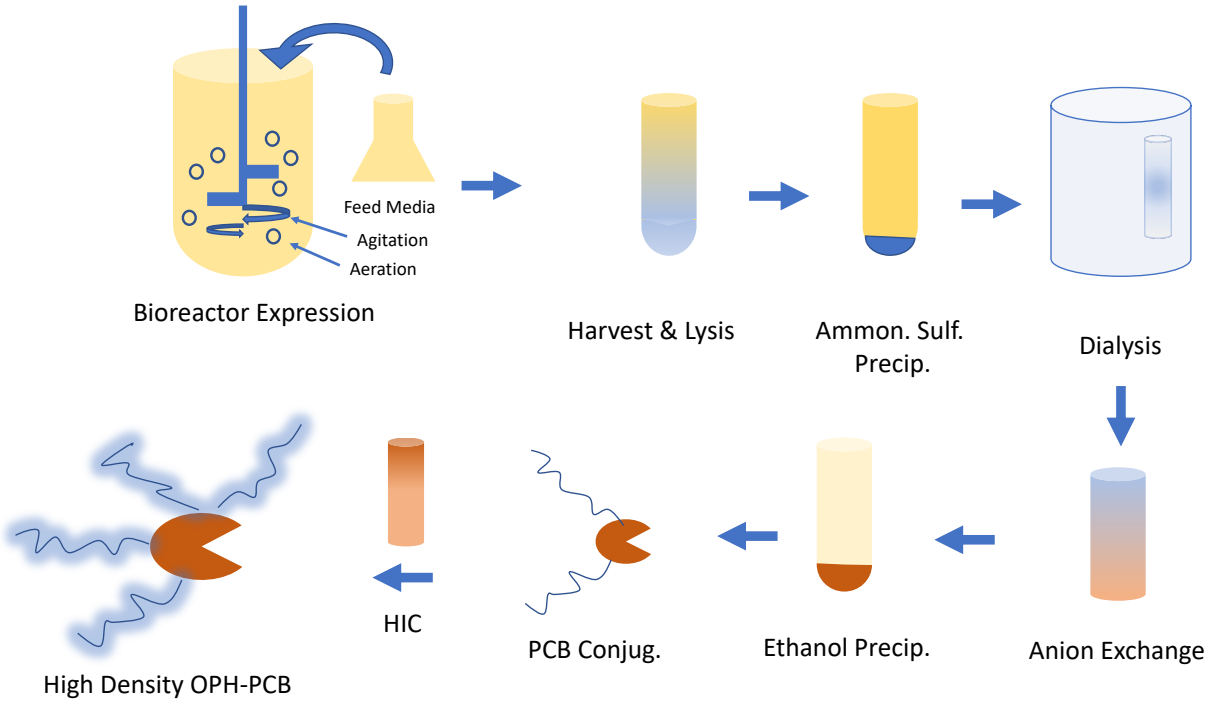

Figure 5-1: Flow Chart of Scaled Up OPH expression, purification, and conjugation. OPH Expressed in a 2L Fed Batch bioreactor with aeration and agitation. Cultures were harvested, lysed, and clarified. Then protein was precipitated with ammonium sulfate and redissolved. Residual salt was removed by dialysis. Protein was applied to captoQ anion exchange column. Lipids were removed by ethanol precipitation. PCB was conjugated using AMAS crosslinker and purified using captoButyl hydrophobic interaction chromatography (HIC) to achieve high density PCB-OPH conjugates.

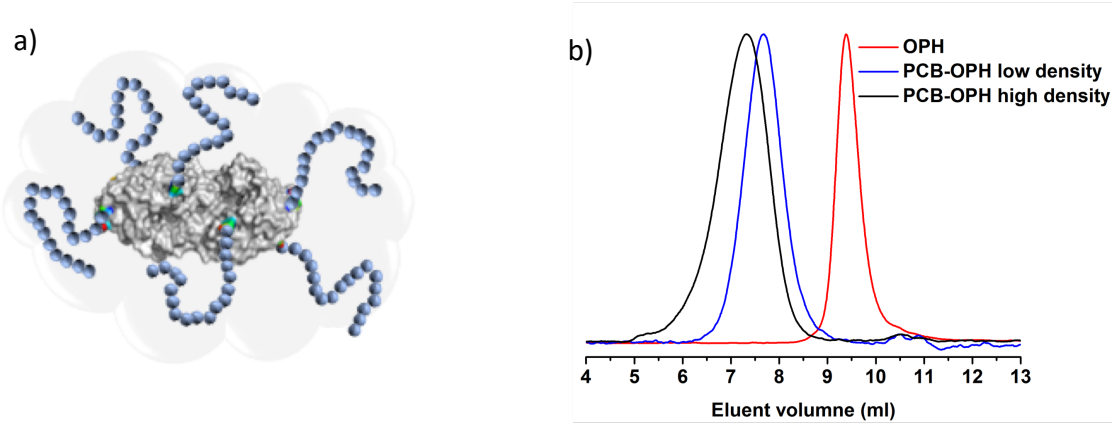

Figure 5-2: a) Schematic of PCB conjugation to OPH demonstrating the available conjugation sites. Low and high density indicates few and many PCB polymers conjugated to the surface of OPH. b) Gel Permeation Chromatography for unconjugated OPH, low density PCB-OPH conjugates, and high density PCB-OPH conjugates.

	Km (mM)	Vmax (mM min)	Kcat (S^{-1})	Kcat/Km (M^{-1} S^{-1})
OPH	0.226	0.620	8.06×10^3	3.57×10^7
PCB-OPH (low density)	0.157	0.500	6.50×10^3	4.14×10^7
PCB-OPH (high density)	0.142	0.453	5.89×10^3	4.15×10^7

Table 5-1: Michaelis-Menten enzyme kinetic parameters for paraoxon catalyzed by OPH, low density conjugated PCB-OPH, and high-density conjugated PCB-OPH

CONCLUSIONS

The determinants of immunogenicity are of critical importance for the development of safe biotherapeutics by design. PEG, as the current gold standard of inert materials, has been hindered by immunogenic responses when conjugated to immunogenic proteins, preventing its safe use in the clinic. Previous studies have demonstrated that zwitterionic polymers, defined by alternating positive and negative charged moieties, exhibit reduced immunogenicity compared to PEG, likely due to their ultra-hydrophilic and low fouling properties. However, polymer-based approach requires chemical conjugation followed by purification. As a result, biologic therapeutics has become a major area of exploration. Specifically, advances in genetic engineering make protein-based therapeutics commonplace. The protein synthesis pathways also facilitate linkage of multiple protein domains, providing an alternative to the chemical linkage of polymers to proteins. Therefore, it would be advantageous to design a polymer-mimicking peptide linked to a protein therapeutic by genetic engineering. Herein, we designed a de novo low immunogenicity zwitterionic polymer-mimicking peptide fusion protein. To design a zwitterionic peptide, we encoded a DNA to express alternating glutamic acid (E) and lysine (K) residues and integrate random coil inducing amino acids to mimic the unstructured nature of polymers. We uncover that proline (P) containing zwitterionic peptides (termed EKP) are able to recapitulate the circulation enhancing properties of polymers. We demonstrate this effect on two bioactive therapeutic proteins, growth colony-stimulating factor (GCSF) and interferon alpha 2 a (IFN).

Then, we designed several EKX-IFN variants to see the effects of different random coil inducing amino acids on their *in vitro* properties as well as *in vivo* circulation and immunogenicity. EKP and EPKP variants retained their circulation retention properties for multiple injections while exhibiting low immunogenicity. However, EPKP-IFN exhibited significantly reduced *in vitro* activity compared to EKP-IFN. EKP-IFN preserved much of its activity although lower than

unfused IFN. Furthermore, appreciably retained pharmacokinetics and low immunogenicity recommend EKP-IFN as a suitable candidate for future trials.

To better understand the determinants of immunogenicity for EKX variants, we conducted epitope mapping and alanine scanning experiments to elucidate the predominant chemical driving forces of EKX peptides for the design of low immunogenicity peptides. Glutamic acid to alanine substitutions tended to increase antibody binding, while lysine to alanine mutations tended to decrease antibody binding, suggesting that the juxtaposition of E and K was more important factor impacting immunogenicity rather than the specific identity of X. Therefore, we conducted an *in vivo* immunogenicity screen composed of E and K positional variants (i+1 to i+4) and rotational variants of X (P, S, and G). This screen revealed the i+1 EK with no structure disrupting amino acid, i+1 with proline, as well as all i+2, E and K positional variants tend to be lower immunogenicity compared to the other variants. These findings were consistent with the observed results from the genetically engineered EKX variants.

To advance zwitterionic polymer conjugates, we also developed scaled-up expression and purification strategies of polycarboxybetaine (PCB) conjugated organophosphate hydrolase (OPH) to better combat chemical warfare nerve agents. We eliminate OPH-PCB conjugates with exposed hydrophobic moieties using hydrophobic interaction chromatography (HIC) for well-protected OPH-PCB conjugates.

In summary, we designed a novel genetically engineered zwitterionic peptide fusion protein platform to replace PEGylation. The zwitterionic peptide fusion protein platform exhibits similar circulation half-life extension properties as PEG. Moreover, these fusion proteins exhibit low immunogenicity and can be injected multiple times with no significant alterations in the pharmacokinetic profile. Finally, we examined the determinants of the low immunogenicity of

zwitterionic peptides by conducting epitope mapping, alanine scanning, and *in vivo* immunogenicity screening. These approaches yielded new low immunogenic peptides for future applications.

FUTURE DIRECTIONS

Thus far we have demonstrated the increased circulation time of EKX fusion proteins and showed their retained pharmacokinetic profiles for multiple injections, thus suggesting they will not demonstrate an ABC effect. Moreover, the antibody titers against EKX proteins were quite low. Our screen also revealed candidate sequences that demonstrate comparable antibody titers to EK, which showed promising results when conjugated to asparaginase, thereby revealing new low immunogenic candidate sequences. In addition, higher immunogenicity than expected was observed with EKS and EKG, despite being predicted to have low immunogenic responses due to their lower hydrophobicity. We suspect unique structural and hydrogen bonding properties may contribute to this effect as similar glycine content sequences do not exhibit this elevated immunogenicity. These effects also point to an incomplete understanding of peptide hydrophobicity. Experimental methods to characterize amino acid hydrophobicity are inconsistent. There are some clear trends that charged amino acids have greater hydrophilicity while aromatic and some aliphatic residues have greater hydrophobicity. However, other amino acids such as proline, glycine, serine, and aliphatic residues with short side chains are less clear in term of hydrophobicity and hydrogen bonding, and their behavior is dependent on specific experimental conditions.

As these properties are still debated, selecting low immunogenic candidate sequences based on physicochemical properties will likely have variable success. Therefore, it would be highly advantageous to test a greater sequence space with broader physicochemical properties via experimental screening methods. The *in vivo* KLH-EKX immunogenicity testing is particularly informative for twenty or thirty sequences but cannot be used for larger screening efforts as the method requires several animals for each peptide tested. Transforming the assay into an *in vitro*

format, though, would reduce the animal cost enabling the screening of hundreds of peptides simultaneously in 96 well plates. One possible route could be exposing biomaterial antigens to peripheral blood mononuclear cells (PBMCs) and analyzing cytokine responses, which has been done previously (Joubert et al., 2016; Wullner et al., 2010). Alternatively, screens have been done with macrophages to look examine their phenotypic responses to biomaterials (Rostam et al., 2020). However, these alone may not fully predict peptide immunogenicity as they do not fully recapitulate the immune environment. Interesting new studies in antibody development have shown artificial organoid lymph nodes serve as a platform for *in vitro* antibody production suggesting they may better replicate the immune environment. Thus, lymphatic organoids may be useful for *in vitro* peptide immunogenicity screening. These *in vitro* techniques coupled with peptide synthesis may be the pathway to scan a much greater array of peptides to predict immunogenicity, thereby negating the shortcomings of selecting sequences based on physicochemical properties. Even so, the bottleneck of relying on individually synthesized peptides poses a significant constraint limiting the testable peptide quantity to hundreds.

Moving forward, genetically encoded display techniques such as yeast display or phage display may be potential avenues to alleviate the bottleneck of individually produced peptides. These techniques can facilely and rapidly assess at least 10^8 sequences, while simultaneously identifying candidate sequences. Theoretically, a phage display library could be injected several times into mice or introduced into a lymph node organoid to elicit an antibody response targeting the peptide library. Subsequently, panning experiments could probe for elicited antibody responses to select for non-immunogenic sequences. In practice, this is very similar to phage display vaccines. However, phage display vaccines typically only display one antigen or a limited number of antigens, suggesting there may be a limit to the phage display library size that can effectively

screen for immunogenicity. Alternatively, B cell receptors play a key role in the specificity of a mounted immune response and can be the first point of specific recognition for peptide antigens. Therefore, probing the B cell repertoire with a phage display or yeast display library may be a good starting for selecting for non-immunogenic peptides. As the B cell receptor diversity is quite large, the likelihood of a displayed peptide binding an antibody is actually quite high, and thus, drastically increasing the selective pressure for non-binding interactions. Similar methods pairing DNA barcoded peptides and single cell sequencing have successfully probe the B cell receptor repertoire of HIV infected patients suggesting probing the B cell repertoire is feasible (Setliff et al., 2019). As well, phage display methods have been used to probe the T cell receptor repertoire indicating display techniques are sensitive enough to detect specific binding interactions at the cellular and molecular levels (Kula et al., 2019).

These methods to screen for low immunogenic peptides are not only important for zwitterionic peptide design but also can be the basis for important fundamental studies. As mentioned earlier, predictive algorithms have proved not as accurate as once anticipated. A large reason barrier is due to insufficient or highly variable quality of input data. Data obtained by libraries coupled with next-generation sequencing may be able to overcome this hurdle. Coupling these technologies with machine learning techniques could prove powerful in predicting low immunogenic peptides as machine learning does not require input parameters such as the physicochemical properties of the amino acids to predict a particular outcome.

These futuristic exploratory approaches, however, do not underscore the importance of zwitterionic peptides as a benchmark of low immunogenicity. Efforts to drive peptide immunogenicity even lower should not overlook the principles of hydration as a critical design consideration. Furthermore, screening, despite its seemingly infinite capability, in reality, is yet

limited by sequence constraints. Highly variable peptide libraries are not likely to identify the best low immunogenic peptide, but only peptides that are relatively low in immunogenicity. Starting from a constrained peptide such as EKX i+2 variants may be necessary to increase the probability of identifying the best low immunogenicity peptide. These requirements highlight the work presented in this dissertation as a critical bridge for future exploration and as the foundation for ensuing studies.

REFERENCES

Arvedson, T., O'Kelly, J., & Yang, B. B. (2015). Design rationale and development approach for pegfilgrastim as a long-acting granulocyte colony-stimulating factor. *BioDrugs*. https://doi.org/10.1007/s40259-015-0127-4

Bailon, P., Palleroni, A., Schaffer, C. A., Spence, C. L., Fung, W. J., Porter, J. E., … Berthold, W. (2001). Rational design of a potent, long-lasting form of interferon: A 40 kDa branched polyethylene glycol-conjugated interferon α-2a for the treatment of hepatitis C. *Bioconjugate Chemistry*, *12*(2), 195–202. https://doi.org/10.1021/bc000082g

Baker, M. P., Reynolds, H. M., Lumicisi, B., & Bryson, C. J. (2010). Immunogenicity of protein therapeutics: The key causes, consequences and challenges. *Self/Nonself - Immune Recognition and Signaling*, *1*(4), 314–322. https://doi.org/10.4161/self.1.4.13904

Bigley, A. N., Mabanglo, M. F., Harvey, S. P., & Raushel, F. M. (2015). Variants of Phosphotriesterase for the Enhanced Detoxification of the Chemical Warfare Agent VR. *Biochemistry*, *54*(35), 5502–5512. https://doi.org/10.1021/acs.biochem.5b00629

Bogan, A. A., & Thorn, K. S. (1998). Anatomy of hot spots in protein interfaces. *Journal of Molecular Biology*, *280*(1), 1–9. https://doi.org/10.1006/jmbi.1998.1843

Brant, D. A., Miller, W. G., & Flory, P. J. (1967). Conformational energy estimates for statistically coiling polypeptide chains. *Journal of Molecular Biology*, *23*(1), 47–65. https://doi.org/10.1016/S0022-2836(67)80066-4

Breibeck, J., & Skerra, A. (2018). The polypeptide biophysics of proline/alanine-rich sequences (PAS): Recombinant biopolymers with PEG-like properties. *Biopolymers*, *109*(1), 1–12. https://doi.org/10.1002/bip.23069

Brems, D. N. (2008). The kinetics of G-CSF folding. *Protein Science*. https://doi.org/10.1110/ps.0206202

Bryson, C. J., Jones, T. D., & Baker, M. P. (2010). Prediction of Immunogenicity of Therapeutic Proteins. *BioDrugs*, *24*(1), 1–8. https://doi.org/10.2165/11318560-000000000-00000

Calbo, S., Guichard, G., Bousso, P., Muller, S., Kourilsky, P., Briand, J. P., & Abastado, J. P. (1999). Role of peptide backbone in T cell recognition. *Journal of Immunology*, *162*(8), 4657–4662.

Chakrabarti, P., & Chakrabarti, S. (1998). C-H···O hydrogen bond involving proline residues in α-helices. *Journal of Molecular Biology*. https://doi.org/10.1006/jmbi.1998.2199

Chapman, R. G., Ostuni, E., Takayama, S., Holmlin, R. E., Yan, L., & Whitesides, G. M. (2000). Surveying for surfaces that resist the adsorption of proteins [3]. *Journal of the American Chemical Society*. https://doi.org/10.1021/ja000774f

Chen, S., Cao, Z., & Jiang, S. (2009). Ultra-low fouling peptide surfaces derived from natural amino acids. *Biomaterials*, *30*(29), 5892–5896. https://doi.org/10.1016/j.biomaterials.2009.07.001

Chen, S., Yu, F., Yu, Q., He, Y., & Jiang, S. (2006). Strong resistance of a thin crystalline layer of balanced charged groups to protein adsorption. *Langmuir*, *22*(19), 8186–8191. https://doi.org/10.1021/la061012m

Chowell, D., Krishna, S., Becker, P. D., Cocita, C., Shu, J., Tan, X., … Anderson, K. S. (2015). TCR contact residue hydrophobicity is a hallmark of immunogenic CD8+ T cell epitopes. *Proceedings of the National Academy of Sciences of the United States of America*, *112*(14),

E1754–E1762. https://doi.org/10.1073/pnas.1500973112

Cromwell, M. E. M., Hilario, E., & Jacobson, F. (2006). Protein aggregation and bioprocessing. *AAPS Journal*, *8*(3). https://doi.org/10.1208/aapsj080366

Davies, D. R., & Cohen, G. H. (1996). Interactions of protein antigens with antibodies. *Proceedings of the National Academy of Sciences of the United States of America*. https://doi.org/10.1073/pnas.93.1.7

De Almeida, P. E., Ransohoff, J. D., Nahid, A., & Wu, J. C. (2013). Immunogenicity of pluripotent stem cells and their derivatives. *Circulation Research*, *112*(3), 549–561. https://doi.org/10.1161/CIRCRESAHA.111.249243

Dobson, C. M., Šali, A., & Karplus, M. (1998). Protein folding: A perspective from theory and experiment. *Angewandte Chemie - International Edition*. https://doi.org/10.1002/(SICI)1521-3773(19980420)37:7<868::AID-ANIE868>3.0.CO;2-H

Dutta, S., & Bhattacharyya, D. (2001). Size of unfolded and dissociated subunits versus that of native multimeric proteins. *Journal of Biological Physics*, *27*(1), 59–71. https://doi.org/10.1023/A:1011826525684

Eddleston, M., Buckley, N. A., Eyer, P., & Dawson, A. H. (2008). Management of acute organophosphorus pesticide poisoning. *The Lancet*, *371*(9612), 597–607. https://doi.org/10.1016/S0140-6736(07)61202-1

Fadeel, B. (2019). Hide and seek: Nanomaterial interactions with the immune system. *Frontiers in Immunology*, *10*(FEB), 1–10. https://doi.org/10.3389/fimmu.2019.00133

Finco, O., & Rappuoli, R. (2014). Designing vaccines for the twenty-first century society.

Frontiers in Immunology, *5*(JAN), 1–6. https://doi.org/10.3389/fimmu.2014.00012

Fiorucci, S., & Zacharias, M. (2010). Prediction of protein-protein interaction sites using electrostatic desolvation profiles. *Biophysical Journal*, *98*(9), 1921–1930. https://doi.org/10.1016/j.bpj.2009.12.4332

FISHBURN, C. S. (2008). The Pharmacology of PEGylation: Balancing PD with PK to Generate Novel Therapeutics. *JOURNAL OF PHARMACEUTICAL SCIENCES*, *97*(10), 4167–4183. https://doi.org/10.1002/jps

Flower, D. R. (2003). Towards in silico prediction of immunogenic epitopes. *Trends in Immunology*, *24*(12), 667–674. https://doi.org/10.1016/j.it.2003.10.006

Fukunaga, A., & Tsumoto, K. (2013). Improving the affinity of an antibody for its antigen via long-range electrostatic interactions. *Protein Engineering, Design and Selection*, *26*(12), 773–780. https://doi.org/10.1093/protein/gzt053

Govrin, R., Tcherner, S., Obstbaum, T., & Sivan, U. (2018). Zwitterionic Osmolytes Resurrect Electrostatic Interactions Screened by Salt. *Journal of the American Chemical Society*. https://doi.org/10.1021/jacs.8b07771

Gray, T. M., & Matthews, B. W. (1984). Intrahelical hydrogen bonding of serine, threonine and cysteine residues within α-helices and its relevance to membrane-bound proteins. *Journal of Molecular Biology*. https://doi.org/10.1016/0022-2836(84)90446-7

Gummert, J. F., Ikonen, T., & Morris, R. E. (1999). Newer immunosuppressive drugs: A review. *Journal of the American Society of Nephrology*, *10*(6), 1366–1380.

Hogrefe, H. H., Kaumaya, P. T. P., & Goldberg, E. (1989). Immunogenicity of synthetic peptides

corresponding to flexible and antibody-accessible segments of mouse lactate dehydrogenase (LDH)-C4. *Journal of Biological Chemistry*, *264*(18), 10513–10519.

Hower, J. C., Bernards, M. T., Chen, S., Tsao, H. K., Sheng, Y. J., & Jiang, S. (2009). Hydration of "Nonfouling" functional groups. *Journal of Physical Chemistry B*, *113*(1), 197–201. https://doi.org/10.1021/jp8065713

Imai, K., & Mitaku, S. (2005). Mechanisms of secondary structure breakers in soluble proteins. *Biophysics*, *1*, 55–65. https://doi.org/10.2142/biophysics.1.55

Ishida, T., & Kiwada, H. (2013). Anti －polyethyleneglycol Antibody Response to PEGylated Substances. *Biol. Pharm. Bull.*, *36*(6), 889–891.

Ivanov, I. I., Schelonka, R. L., Zhuang, Y., Gartland, G. L., Zemlin, M., & Schroeder, H. W. (2005). Development of the Expressed Ig CDR-H3 Repertoire Is Marked by Focusing of Constraints in Length, Amino Acid Use, and Charge That Are First Established in Early B Cell Progenitors. *The Journal of Immunology*, *174*(12), 7773–7780. https://doi.org/10.4049/jimmunol.174.12.7773

Jespersen, M. C., Mahajan, S., Peters, B., Nielsen, M., & Marcatili, P. (2019). Antibody specific B-cell epitope predictions: Leveraging information from antibody-antigen protein complexes. *Frontiers in Immunology*, *10*(FEB), 1–10. https://doi.org/10.3389/fimmu.2019.00298

Joubert, M. K., Deshpande, M., Yang, J., Reynolds, H., Bryson, C., Fogg, M., … Jawa, V. (2016). Use of in vitro assays to assess immunogenicity risk of antibody-based biotherapeutics. *PLoS ONE*, *11*(8), 1–22. https://doi.org/10.1371/journal.pone.0159328

Kay, B. K., Williamson, M. P., & Sudol, M. (2000). The importance of being proline: the

interaction of proline-rich motifs in signaling proteins with their cognate domains. *The FASEB Journal*. https://doi.org/10.1096/fasebj.14.2.231

Keil, B. (1992). Specificity of Proteolysis. In *Specificity of Proteolysis*. https://doi.org/10.1007/978-3-642-48380-6

Kolaskar, A. S., & Tongaonkar, P. C. (1990). A semi-empirical method for prediction of antigenic determinants on protein antigens. *FEBS Letters*, *276*(1–2), 172–174. https://doi.org/10.1016/0014-5793(90)80535-Q

Kula, T., Dezfulian, M. H., Wang, C. I., Abdelfattah, N. S., Hartman, Z. C., Wucherpfennig, K. W., … Elledge, S. J. (2019). T-Scan: A Genome-wide Method for the Systematic Discovery of T Cell Epitopes. *Cell*, *178*(4), 1016-1028.e13. https://doi.org/10.1016/j.cell.2019.07.009

Leader, B., Baca, Q. J., & Golan, D. E. (2008). Protein therapeutics: A summary and pharmacological classification. *Nature Reviews Drug Discovery*, *7*(1), 21–39. https://doi.org/10.1038/nrd2399

Levin, D., Golding, B., Strome, S. E., & Sauna, Z. E. (2015). Fc fusion as a platform technology: Potential for modulating immunogenicity. *Trends in Biotechnology*, *33*(1), 27–34. https://doi.org/10.1016/j.tibtech.2014.11.001

Li, B., Yuan, Z., Hung, H. C., Ma, J., Jain, P., Tsao, C., … Jiang, S. (2018). Revealing the Immunogenic Risk of Polymers. *Angewandte Chemie - International Edition*. https://doi.org/10.1002/anie.201808615

Liu, E. J., & Jiang, S. (2018). Expressing a Monomeric Organophosphate Hydrolase as an EK Fusion Protein [Research-article]. *Bioconjugate Chemistry*, *29*(11), 3686–3690.

https://doi.org/10.1021/acs.bioconjchem.8b00607

Liu, E. J., Sinclair, A., Keefe, A. J., Nannenga, B. L., Coyle, B. L., Baneyx, F., & Jiang, S. (2015). EKylation: Addition of an Alternating-Charge Peptide Stabilizes Proteins. *Biomacromolecules*, *16*(10), 3357–3361. https://doi.org/10.1021/acs.biomac.5b01031

Marqusee, S., & Baldwin, R. L. (1987). Helix stabilization by Glu-...Lys+ salt bridges in short peptides of de novo design. *Proceedings of the National Academy of Sciences of the United States of America*. https://doi.org/10.1073/pnas.84.24.8898

Martin, D. A., Bradl, H., Collins, T. J., Roth, E., Jäck, H.-M., & Wu, G. E. (2003). Selection of Ig μ Heavy Chains by Complementarity-Determining Region 3 Length and Amino Acid Composition. *The Journal of Immunology*, *171*(9), 4663–4671. https://doi.org/10.4049/jimmunol.171.9.4663

Matthews, S. J., & McCoy, C. (2004). Peginterferon alfa-2a: A review of approved and investigational uses. *Clinical Therapeutics*. https://doi.org/10.1016/S0149-2918(04)90173-7

Maurizi, M. R. (1992). Proteases and protein degradation in Escherichia coli. *Experientia*. https://doi.org/10.1007/BF01923511

McCoy, A. J., Chandana Epa, V., & Colman, P. M. (1997). Electrostatic complementarity at protein/protein interfaces. *Journal of Molecular Biology*, *268*(2), 570–584. https://doi.org/10.1006/jmbi.1997.0987

Mihiri Shashikala, H. B., Chakravorty, A., & Alexov, E. (2019). Modeling electrostatic force in protein-protein recognition. *Frontiers in Molecular Biosciences*, *6*(SEP), 1–11. https://doi.org/10.3389/fmolb.2019.00094

Molineux, G. (2005). The Design and Development of Pegfilgrastim (PEG-rmetHuG-CSF, Neulasta®). *Current Pharmaceutical Design*. https://doi.org/10.2174/1381612043452613

Moreira, I. S., Fernandes, P. A., & Ramos, M. J. (2007). Hot spots - A review of the protein-protein interface determinant amino-acid residues. *Proteins: Structure, Function and Genetics*. https://doi.org/10.1002/prot.21396

Nielsen, M., Lund, O., Buus, S., & Lundegaard, C. (2010). MHC Class II epitope predictive algorithms. *Immunology*, *130*(3), 319–328. https://doi.org/10.1111/j.1365-2567.2010.03268.x

Novikov, B. N., Grimsley, J. K., Kern, R. J., Wild, J. R., & Wales, M. E. (2010). Improved pharmacokinetics and immunogenicity profile of organophosphorus hydrolase by chemical modification with polyethylene glycol. *Journal of Controlled Release*, *146*(3), 318–325. https://doi.org/10.1016/j.jconrel.2010.06.003

Nowinski, A. K., Sun, F., White, A. D., Keefe, A. J., & Jiang, S. (2012). Sequence, Structure, and Function of Peptide Self-assembled Monolayers Ann. *Journal of American Chemistry Society*, *134*(13). https://doi.org/10.1038/jid.2014.371

Nozaki, Y., & Tanford, C. (1971). The Solubility of Amino in Aqueous Ethanol Acids and Two Glycine Dioxane Solutions Peptides. *The Journal of Biological Chemistry*.

O'Brien, C., Flower, D. R., & Feighery, C. (2008). Peptide length significantly influences in vitro affinity for MHC class II molecules. *Immunome Research*, *4*(1), 1–7. https://doi.org/10.1186/1745-7580-4-6

Okanny, C. C., Durosimi, M. A., Chukwuani, C. M., Njoku, O. S., Akinola, N. O., Herrada, S. C., … Akinsete, I. (2000). Interferon alfa-2a (Roferon-A) monotherapy in chronic myelogenous leukemia: a pilot study in Nigerian patients in early chronic phase. *West African Journal of Medicine*.

Ostuni, E., Chapman, R. G., Holmlin, R. E., Takayama, S., & Whitesides, G. M. (2001). A survey of structure-property relationships of surfaces that resist the adsorption of protein. *Langmuir*. https://doi.org/10.1021/la010384m

Podust, V. N., Balan, S., Sim, B. C., Coyle, M. P., Ernst, U., Peters, R. T., & Schellenberger, V. (2016). Extension of in vivo half-life of biologically active molecules by XTEN protein polymers. *Journal of Controlled Release*, *240*, 52–66. https://doi.org/10.1016/j.jconrel.2015.10.038

Ponomarenko, J., Bui, H. H., Li, W., Fusseder, N., Bourne, P. E., Sette, A., & Peters, B. (2008). ElliPro: A new structure-based tool for the prediction of antibody epitopes. *BMC Bioinformatics*, *9*, 1–8. https://doi.org/10.1186/1471-2105-9-514

Qi Yang, S. L. (2015). 乳鼠心肌提取 HHS Public Access. *Wiley Interdiscip Rev Nanomed Nanobiotechnol*, *7*(5), 655–677. https://doi.org/10.1016/j.physbeh.2017.03.040

Reddy Chichili, V. P., Kumar, V., & Sivaraman, J. (2013). Linkers in the structural biology of protein-protein interactions. *Protein Science*, *22*(2), 153–167. https://doi.org/10.1002/pro.2206

Rosenberg, A. S. (2006). Effects of protein aggregates: An Immunologic perspective. *AAPS Journal*, *8*(3), 501–507. https://doi.org/10.1208/aapsj080359

Rostam, H. M., Fisher, L. E., Hook, A. L., Burroughs, L., Luckett, J. C., Figueredo, G. P., … Ghaemmaghami, A. M. (2020). Immune-Instructive Polymers Control Macrophage Phenotype and Modulate the Foreign Body Response In Vivo. *Matter*, *2*(6), 1564–1581. https://doi.org/10.1016/j.matt.2020.03.018

Sammond, D. W., Payne, C. M., Brunecky, R., Himmel, M. E., Crowley, M. F., & Beckham, G. T. (2012). Cellulase linkers are optimized based on domain type and function: insights from sequence analysis, biophysical measurements, and molecular simulation. *PloS One*, *7*(11). https://doi.org/10.1371/journal.pone.0048615

Sant'Angelo, D. B., Robinson, E., Janeway, C. A., & Denzin, L. K. (2002). Recognition of core and flanking amino acids of MHC class II-bound peptides by the T cell receptor. *European Journal of Immunology*, *32*(9), 2510–2520. https://doi.org/10.1002/1521-4141(200209)32:9<2510::AID-IMMU2510>3.0.CO;2-Q

Sauna, Z. E., Lagassé, H. A. D., Alexaki, A., Simhadri, V. L., Katagiri, N. H., Jankowski, W., & Kimchi-Sarfaty, C. (2017). Recent advances in (therapeutic protein) drug development. *F1000Research*, *6*. https://doi.org/10.12688/f1000research.9970.1

Saunders, R. N., Metcalfe, M. S., & Nicholson, M. L. (2001). Rapamycin in transplantation: A review of the evidence. *Kidney International*, *59*(1), 3–16. https://doi.org/10.1046/j.1523-1755.2001.00460.x

Schellenberger, V., Wang, C. W., Geething, N. C., Spink, B. J., Campbell, A., To, W., … Stemmer, W. P. C. (2009). A recombinant polypeptide extends the in vivo half-life of peptides and proteins in a tunable manner. *Nature Biotechnology*, *27*(12), 1186–1190. https://doi.org/10.1038/nbt.1588

Schimmel, P. R., & Flory, P. J. (1968). Conformational energies and configurational statistics of copolypeptides containing l-proline. *Journal of Molecular Biology*, *34*(1), 105–120. https://doi.org/10.1016/0022-2836(68)90237-4

SCHIMMEL, P. R., & FLORY, P. J. (1967). CONFORMA TIONAL ENERGY AND CONFIGURATIONAL STATISTICS OF POLY-L-PROLINE. *Proceedings of the National Academy of Sciences*, *58*, 52–59.

Schlapschy, M., Binder, U., Börger, C., Theobald, I., Wachinger, K., Kisling, S., … Skerra, A. (2013). PASylation: A biological alternative to PEGylation for extending the plasma half-life of pharmaceutically active proteins. *Protein Engineering, Design and Selection*, *26*(8), 489–501. https://doi.org/10.1093/protein/gzt023

Schlapschy, M., Theobald, I., Mack, H., Schottelius, M., Wester, H. J., & Skerra, A. (2007). Fusion of a recombinant antibody fragment with a homo-amino-acid polymer: Effects on biophysical properties and prolonged plasma half-life. *Protein Engineering, Design and Selection*, *20*(6), 273–284. https://doi.org/10.1093/protein/gzm020

Schlosser, M., Wilhelm, L., Urban, G., Ziegler, B., Ziegler, M., & Zippel, R. (2002). Immunogenicity of polymeric implants: Long-term antibody response against polyester (Dacron) following the implantation of vascular prostheses into LEW.1A rats. *Journal of Biomedical Materials Research*, *61*(3), 450–457. https://doi.org/10.1002/jbm.10096

Schmidt, J., Guillaume, P., Dojcinovic, D., Karbach, J., Coukos, G., & Luescher, I. (2017). In silico and cell-based analyses reveal strong divergence between prediction and observation of T-cell-recognized tumor antigen T-cell epitopes. *Journal of Biological Chemistry*, *292*(28), 11840–11849. https://doi.org/10.1074/jbc.M117.789511

Schmidt, M. M., Townson, S. A., Andreucci, A. J., King, B. M., Schirmer, E. B., Murillo, A. J., … Barnes, T. M. (2013). Crystal structure of an HSA/FcRn complex reveals recycling by competitive mimicry of HSA ligands at a pH-dependent hydrophobic interface. *Structure*, *21*(11), 1966–1978. https://doi.org/10.1016/j.str.2013.08.022

Scholz, M., Engel, C., Apt, D., Sankar, S. L., Goldstein, E., & Loeffler, M. (2009). Pharmacokinetic and pharmacodynamic modelling of the novel human granulocyte colony-stimulating factor derivative Maxy-G34 and pegfilgrastim in rats. *Cell Proliferation*. https://doi.org/10.1111/j.1365-2184.2009.00641.x

Schweitzer-Stenner, R. (2012). Conformational propensities and residual structures in unfolded peptides and proteins. *Molecular BioSystems*, *8*(1), 122–133. https://doi.org/10.1039/c1mb05225j

Setliff, I., Shiakolas, A. R., Pilewski, K. A., Murji, A. A., Mapengo, R. E., Janowska, K., … Georgiev, I. S. (2019). High-Throughput Mapping of B Cell Receptor Sequences to Antigen Specificity. *Cell*, *179*(7), 1636-1646.e15. https://doi.org/10.1016/j.cell.2019.11.003

Shao, Q. (2020). Effect of conjugated (EK)10peptide on structural and dynamic properties of ubiquitin protein: A molecular dynamics simulation study. *Journal of Materials Chemistry B*. https://doi.org/10.1039/d0tb00664e

Sharma, B. (2007). Immunogenicity of therapeutic proteins. Part 3: Impact of manufacturing changes. *Biotechnology Advances*, *25*(3), 325–331. https://doi.org/10.1016/j.biotechadv.2007.01.007

Smith, J., McMullen, P., Yuan, Z., Pfaendtner, J., & Jiang, S. (2020). Elucidating Molecular

Design Principles for Charge-Alternating Peptides. *Biomacromolecules*. https://doi.org/10.1021/acs.biomac.9b01191

Soni, K. S., Desale, S. S., & Bronich, T. K. (2016). Nanogels: an overview of properties, biomedical applications and obstacles to clinical translation. *Journal of Controlled Release*, *240*, 109–126. https://doi.org/10.1016/j.physbeh.2017.03.040

Strohl, W. R. (2015). Fusion Proteins for Half-Life Extension of Biologics as a Strategy to Make Biobetters. *BioDrugs*, *29*(4), 215–239. https://doi.org/10.1007/s40259-015-0133-6

Sundy, J. S., Baraf, H. S. B., Yood, R. A., Edwards, N. L., Gutierrez-Urena, S. R., Treadwell, E. L., … Becker, M. A. (2011). Efficacy and tolerability of pegloticase for the treatment of chronic gout in patients refractory to conventional treatment: Two randomized controlled trials. *JAMA - Journal of the American Medical Association*, *306*(7), 711–720. https://doi.org/10.1001/jama.2011.1169

Swierczewska, M., Lee, K. C., & Lee, S. (2015). What is the future of PEGylated therapies? *Expert Opin. Emerg. Drugs*, *20*(4), 255–269. https://doi.org/10.1517/14728214.2015.1113254

Swindells, M. B., Macarthur, M. W., & Thornton, J. M. (n.d.). *of known structures*. *2*(7), 596–603.

T. Lissitchkov, D. Rudin, J. Fruebis, K. Rice, S. Poloskey, L. Frohlich, S. Katragadda, K. K. (2019). PB0246 - Safety, Tolerability, and Pharmacokinetics of Repeat Dosing with BIVV001 in Patients with Severe Hemophilia A: Results of an Interim Analysis from a Phase 1 Study.

Thomson, C. A., Olson, M., Jackson, L. M., & Schrader, J. W. (2012). A Simplified Method for the Efficient Refolding and Purification of Recombinant Human GM-CSF. *PLoS ONE*.

https://doi.org/10.1371/journal.pone.0049891

Tripathi, N. K., Shrivastva, A., Biswal, K. C., & Rao, P. V. L. (2008). TITLE: Media optimization for dengue protein production. *Industrial Biotechnology*, *5*(3), 179–183. Retrieved from https://pdfs.semanticscholar.org/a1d1/e724aa43d83c6eb2a9f865ab31f9faa63716.pdf

Trovaslet-Leroy, M., Musilova, L., Renault, F., Brazzolotto, X., Misik, J., Novotny, L., … Nachon, F. (2011). Organophosphate hydrolases as catalytic bioscavengers of organophosphorus nerve agents. *Toxicology Letters*, *206*(1), 14–23. https://doi.org/10.1016/j.toxlet.2011.05.1041

Tsai, C. J., Lin, S. L., Wolfson, H. J., & Nussinov, R. (1997). Studies of protein-protein interfaces: A statistical analysis of the hydrophobic effect. *Protein Science*, *6*(1), 53–64. https://doi.org/10.1002/pro.5560060106

Turecek, P. L., Bossard, M. J., Schoetens, F., & Ivens, I. A. (2016). PEGylation of Biopharmaceuticals: A Review of Chemistry and Nonclinical Safety Information of Approved Drugs. *Journal of Pharmaceutical Sciences*, *105*(2), 460–475. https://doi.org/10.1016/j.xphs.2015.11.015

Van Rosmalen, M., Krom, M., & Merkx, M. (2017). Tuning the Flexibility of Glycine-Serine Linkers to Allow Rational Design of Multidomain Proteins. *Biochemistry*. https://doi.org/10.1021/acs.biochem.7b00902

Vargas-Madrazo, E., Lara-Ochoa, F., & Almagro, J. C. (1995). Canonical structure repertoire of the antigen-binding site of immunoglobulins suggests strong geometrical restrictions associated to the mechanism of immune recognition. *Journal of Molecular Biology*, *254*(3),

497–504. https://doi.org/10.1006/jmbi.1995.0633

Wales, M. E., & Reeves, T. E. (2012). Organophosphorus hydrolase as an in vivo catalytic nerve agent bioscavenger. *Drug Testing and Analysis*, *4*(3–4), 271–281. https://doi.org/10.1002/dta.381

Wang, Z., Plaxco, K. W., & Makarov, D. E. (2007). Influence of local and residual structures on the scaling behavior and dimensions of unfolded proteins. *Biopolymers*. https://doi.org/10.1002/bip.20747

Webber, M. J., Appel, E. A., Vinciguerra, B., Cortinas, A. B., Thapa, L. S., Jhunjhunwala, S., … Anderson, D. G. (2016). Supramolecular PEGylation of biopharmaceuticals. *Proceedings of the National Academy of Sciences*, *113*(50), 14189–14194. https://doi.org/10.1073/pnas.1616639113

Werle, M., & Bernkop-Schnürch, A. (2006). Strategies to improve plasma half life time of peptide and protein drugs. *Amino Acids*, *30*(4), 351–367. https://doi.org/10.1007/s00726-005-0289-3

White, A. D., Huang, W., & Jiang, S. (2012). Role of nonspecific interactions in molecular chaperones through model-based bioinformatics. *Biophysical Journal*, *103*(12), 2484–2491. https://doi.org/10.1016/j.bpj.2012.10.040

White, A. D., Keefe, A. J., Ella-Menye, J. R., Nowinski, A. K., Shao, Q., Pfaendtner, J., & Jiang, S. (2013). Free energy of solvated salt bridges: A simulation and experimental study. *Journal of Physical Chemistry B*, *117*(24), 7254–7259. https://doi.org/10.1021/jp4024469

White, A. D., Nowinski, A. K., Huang, W., Keefe, A. J., Sun, F., & Jiang, S. (2012). Decoding nonspecific interactions from nature. *Chemical Science*, *3*(12), 3488–3494.

https://doi.org/10.1039/c2sc21135a

Woody, R. W. (2010). Circular Dichroism of Intrinsically Disordered Proteins. In *Instrumental Analysis of Intrinsically Disordered Proteins: Assessing Structure and Conformation*. https://doi.org/10.1002/9780470602614.ch10

Wullner, D., Zhou, L., Bramhall, E., Kuck, A., Goletz, T. J., Swanson, S., … Jawa, V. (2010). Considerations for optimization and validation of an in vitro PBMC derived T cell assay for immunogenicity prediction of biotherapeutics. *Clinical Immunology*, *137*(1), 5–14. https://doi.org/10.1016/j.clim.2010.06.018

Yang, Q., Jacobs, T. M., McCallen, J. D., Moore, D. T., Huckaby, J. T., Edelstein, J. N., & Lai, S. K. (2016). Polyethylene Glycol (PEG) in the General Population. *Anal Chem*, *88*(23), 11804–11812. https://doi.org/10.1021/acs.analchem.6b03437.Analysis

Zhang, L., Cao, Z., Bai, T., Carr, L., Ella-Menye, J. R., Irvin, C., … Jiang, S. (2013). Zwitterionic hydrogels implanted in mice resist the foreign-body reaction. *Nature Biotechnology*, *31*(6), 553–556. https://doi.org/10.1038/nbt.2580

Zhang, P., Jain, P., Tsao, C., Sinclair, A., Sun, F., Hung, H. C., … Jiang, S. (2016). Butyrylcholinesterase nanocapsule as a long circulating bioscavenger with reduced immune response. *Journal of Controlled Release*, *230*, 73–78. https://doi.org/10.1016/j.jconrel.2016.04.008

Zhang, P., Sun, F., Tsao, C., Liu, S., Jain, P., Sinclair, A., … Jiang, S. (2015). Zwitterionic gel encapsulation promotes protein stability, enhances pharmacokinetics, and reduces immunogenicity. *Proceedings of the National Academy of Sciences*, *112*(39), 12046–12051.

https://doi.org/10.1073/pnas.1512465112

Zhang, Z., Witham, S., & Alexov, E. (2011). On the role of electrostatics in protein-protein interactions. *Physical Biology*, *8*(3). https://doi.org/10.1088/1478-3975/8/3/035001

Zhao, H. L., Yao, X. Q., Xue, C., Wang, Y., Xiong, X. H., & Liu, Z. M. (2008). Increasing the homogeneity, stability and activity of human serum albumin and interferon-α2b fusion protein by linker engineering. *Protein Expression and Purification*. https://doi.org/10.1016/j.pep.2008.04.013

Zheng, J., Li, L., Chen, S., & Jiang, S. (2004). Molecular simulation study of water interactions with oligo (ethylene glycol)-terminated alkanethiol self-assembled monolayers. *Langmuir*, *20*(20), 8931–8938. https://doi.org/10.1021/la036345n

Zhu, C., Gao, Y., Li, H., Meng, S., Li, L., Francisco, J. S., & Zeng, X. C. (2016). Characterizing hydrophobicity of amino acid side chains in a protein environment via measuring contact angle of a water nanodroplet on planarpeptide network. *Proceedings of the National Academy of Sciences of the United States of America*. https://doi.org/10.1073/pnas.1616138113